2019•2020

Faculteit Industriële ingenieurswetenschappen

master in de industriële wetenschappen: energie

Masterthesis

Modelling the impact of DERs in LV grids

PROMOTOR :

Prof. dr. ir. Wilmar MARTINEZ

PROMOTOR :

Dr. ing. David TOPOLANEK

Arjen Mentens

Scriptie ingediend tot het behalen van de graad van master in de industriële wetenschappen: energie, afstudeerrichting automatisering

Gezamenlijke opleiding UHasselt en KU Leuven

2019•2020

Faculteit Industriële ingenieurswetenschappen

master in de industriële wetenschappen: energie

Masterthesis

Modelling the impact of DERs in LV grids

PROMOTOR :

Prof. dr. ir. Wilmar MARTINEZ

PROMOTOR :

Dr. ing. David TOPOLANEK

Arjen Mentens

Scriptie ingediend tot het behalen van de graad van master in de industriële wetenschappen: energie, afstudeerrichting automatisering

UHASSELT

KU LEUVEN

Deze masterproef werd geschreven tijdens de COVID-19 crisis in 2020. Deze wereldwijde gezondheidscrisis heeft mogelijk een impact gehad op de opdracht, de onderzoekshandelingen en de onderzoeksresultaten.

Preface

My interest in the renewable energy sector was one of the main reasons for writing this thesis. In this sector, a lot of progress is made every day and I am glad to be a part of this progress for Brno University of Technology (BUT).

At first, the outbreak of COVID-19 did not seem to have an impact on this thesis. Later on, it became clear that communicating via mail or online meetings are an obstacle when working with simulation models. Not being able to communicate in real life made it difficult to interpret each other and discuss results and issues. Despite this, it was still an exciting experience to develop the simulation model for BUT.

First, I would like to thank dr. ing. David Topolánek for assisting me throughout the semester and providing me with the necessary feedback regarding the interpretation and implementation methods of European standards and regulations using MATLAB / Simulink. Second, I would like to thank prof. dr. ir. Wilmar Martinez for giving me the much appreciated and constructive feedback for writing my thesis. Writing this thesis gave me insight in how to translate documents into a working simulation model. It also taught me to be self-critical and to question simulation results, even though they may seem correct. The combination of going on Erasmus and the COVID-19 outbreak caused a rather unusual situation. Therefore, I would like to thank my family for supporting me throughout this semester.

Contents

List of Figures

List of Tables

Acronyms

BESS battery energy storage system. 29

CHP combined heat and power. 31

DB dead-band. 29, 38

DER distributed energy resource. 15, 19–21, 23, 24, 27, 29, 33, 48, 53, 67, 68

DERMS DER management system. 29

DSM demand side management. 19, 23, 30, 67

DSO Distribution System Operator. 15, 19, 23, 24, 29, 41, 43, 44, 47, 50, 52, 53

DVCN dynamic voltage control need. 24

FRT fault-ride-through. 55, 57

LV low-voltage. 19, 23, 28, 29, 67, 68

LVCN local voltage control need. 24

MV medium-voltage. 23, 25, 29, 38, 67

NaN Not a Number. 58

OLTC on-load tap changer. 19, 23–25, 27, 67

P active power. 23, 26, 28, 29, 37–39, 41, 47, 48, 50, 51, 53, 59–61, 67

PF power factor. 50, 51, 59

PGM power-generating module. 31, 37–41, 48, 59, 67

POC point of connection. 19, 20, 26, 30, 40, 51, 52

PV photovoltaic. 23, 26–29, 33–35, 37, 39, 41, 51, 57, 67

Q reactive power. 23, 26, 28, 29, 41, 49–52, 59–61, 67

RER renewable energy resource. 35, 67

ROCOF rate of change of frequency. 40, 44, 55, 57, 68

TSO Transmission System Operator. 32, 37, 40

Wp Watt-peak. 33

ZOH zero-order hold. 53

Abstract

Distribution System Operators (DSOs) are challenged with an increase in grid events due to the implementation of distributed energy resources (DERs). Voltage levels can vary at the point of connection and are currently not evaluated by DSOs. Therefore, Brno University of Technology is working together with DSO E.ON Distribuce to train operators to better understand grid dynamics and make appropriate decisions in case of grid events. In today's grid, a great amount of inverter-based DERs are connected. Inverters were mainly designed to supply power without considering grid dynamics. This thesis focuses on developing a model of inverter-based DERs for training purposes. The model aims to help operators to simulate grid events and study the impact of DERs to the grid with respect to different settings of integrated support functions.

To better understand why grid issues occur, the literature study focuses on comparing the state-of-the-art grid support and why it does not suffice anymore. According to the current needs, a model is developed in MATLAB/Simulink, conform to European standards and regulations.

Grid dynamics can be evaluated by imitating voltage and frequency deviations. Support functions can either be adjusted according to the situation or turned off. Together with adjustable settings according to DSO request, this model offers flexibility and insight in the capabilities of DERs to solve voltage and frequency issues. Case studies show that the model corresponds to expected behavior and can be used for further development.

Abstract in Dutch

Distributienetbeheerders (DNB's) worden geconfronteerd met een toename van net events als gevolg van de implementatie van distributed energy resources (DER's). Het spanningsniveau op het aansluitingspunt kan variëren en wordt niet geëvalueerd door DNB's. Daarom werkt Brno University of Technology samen met DNB E.ON Distribuce om operatoren op te leiden om juiste beslissingen te nemen in geval van net events. In het huidige net zijn een groot aantal inverter-gebaseerde DER's aangesloten. Inverters zijn voornamelijk ontworpen om stroom te leveren zonder evaluatie van het net. Deze masterproef richt zich op het ontwikkelen van een model van inverter-gebaseerde DER's en is bedoeld om operatoren te helpen om grid events te simuleren en de impact van DER's op het net te bestuderen met betrekking tot verschillende niveaus van geïntegreerde supportfuncties.

Om beter te begrijpen waarom problemen zich voordoen, richt de literatuurstudie zich op het vergelijken van bestaande netondersteuning en hun gebreken. Er wordt een model ontwikkeld in MATLAB / Simulink conform met de Europese regelgeving.

De netdynamiek kan worden geëvalueerd door het simuleren van spannings- en frequentieproblemen. Functies kunnen worden uitgeschakeld of aangepast aan de situatie. Samen met specifieke instellingen voor DNB's biedt dit model flexibiliteit en inzicht in de mogelijkheden van DER's om spannings- en frequentieproblemen op te lossen. Analyses tonen aan dat het model overeenkomt met het verwachte gedrag en kan worden gebruikt voor verdere ontwikkeling.

1 Introduction

1.1 Background

Brno University of Technology (BUT) is the largest engineering university in the Czech Republic. Research topics are wide-ranging from laser technology to distributed energy resources (DERs). For one of their projects, the university is working together with the Distribution System Operator (DSO) E.ON Distribuce to train operators to better understand grid dynamics and make appropriate decisions in case of grid events. Grid events are mainly faults, voltage and frequency deviations. Employing DERs, while they can output active (P) and reactive (Q) power, is becoming one of the most common methods to support grid events [1]–[3]. Consequently, DSOs should improve the grid behaviour, which allows DERs to support the grid in a consistent way.

This project is part of the cooperation between BUT and E.ON Distribuce, with the aim of simulating and visualizing the impact, caused by aforementioned support functions of DERs, on low-voltage (LV) grids. Instead of focusing on demand side management (DSM) to reduce DER injection peaks, this project uses a method based on reducing the injection of the DER itself as a function of the grid conditions [4]. DSM also requires communication through several devices i.e. smart meters to trigger consumption. In addition, most devices do not have smart functions implemented, which makes it necessary to add costly electronics. For this project, only voltage and frequency levels at the point of connection (POC) are evaluated and no communication between DERs is implemented.

1.2 Problem definition

The first issue is due to the increasing integration of DERs. Our distribution grid is becoming a bidirectional lane for power. For instance, instead of solely consuming, households are also supplying an amount of power, mostly due to solar panels and energy storage, which can no longer be ignored [5]. In addition, more inverter-based power plants are being connected to the grid, while the first inverters were mainly designed to supply power without considering distribution grid dynamics. An additional issue of DERs is an increased voltage level at the POC and this is currently not evaluated by DSOs. While electrical appliances are designed to work within voltage and frequency limits, exceeding them may cause damaged household electronics or key appliances in hospitals not functioning properly. on-load tap changers (OLTCs) are currently the only solution for changing the voltage, but this affects the entire LV grid, i.e. both high loaded feeders and feeders with high penetration of DERs, and therefore they do not suffice anymore.

Given the above, we can conclude that additional grid support functions should be implemented in inverters to control voltage levels at the POC [6]. This should be extended from household DERs to inverter-based power plants. Before deployment of support functions, extensive testing needs to be performed in order to prevent errors and optimise effectiveness of implementation. The lack of simulation models makes it more difficult to perform plausible tests [3].

1.3 Goals

The main objective of this thesis is to develop a model of inverter-based DERs for training purposes that helps operators to simulate grid events and study the impact of DERs to the grid with respect to different settings of integrated autonomous functions and different level of DER integration. This will help them make correct decisions in case of real grid events and to better understand grid dynamics when particular safety measures are taken. For example, a safety measure can be disconnecting a DER. The impact on the load flow, voltage and frequency level can then be evaluated. The model has to be self-explanatory, visually appealing and comply with European standards and regulations [6], [7]. This can be done by summarizing the relevant standards and regulations and developing a functional flowchart as a guideline for implementing. Not only developing, but also correcting and optimizing of this flowchart has to be done by comparing the simulation to real grid event results. While this is part of a large project, the deadline of this model was 20 May 2020. By this date, the model had to be completely functional.

1.4 Method

Testing and modelling will be performed in MATLAB/Simulink. The graphical programming environment will make the model visually appealing. Before its implementation, a basic model has to be developed. This model, as illustrated in Figure 1, consists of a voltage source, several loads that simulate household or industrial loads, and one or more DERs. The operator will be able to imitate grid events by switching loads on and off to cause voltage deviations or by setting the frequency level so that the grid dynamics can be evaluated. The voltage in function of the line length provides us insight on the impact of DERs. An active DER will cause a raised voltage near the POC. In Figure 1 this is shown as a positive effect while the voltage level stays within its boundaries for a longer line length. Issues will occur when multiple DERs are connected in an area where they can reinforce each other's behaviour. This may cause the maximum voltage level to be exceeded. To resolve this, DERs should implement functions to support the grid and change their output according to voltage and frequency levels [3], [6], [7].

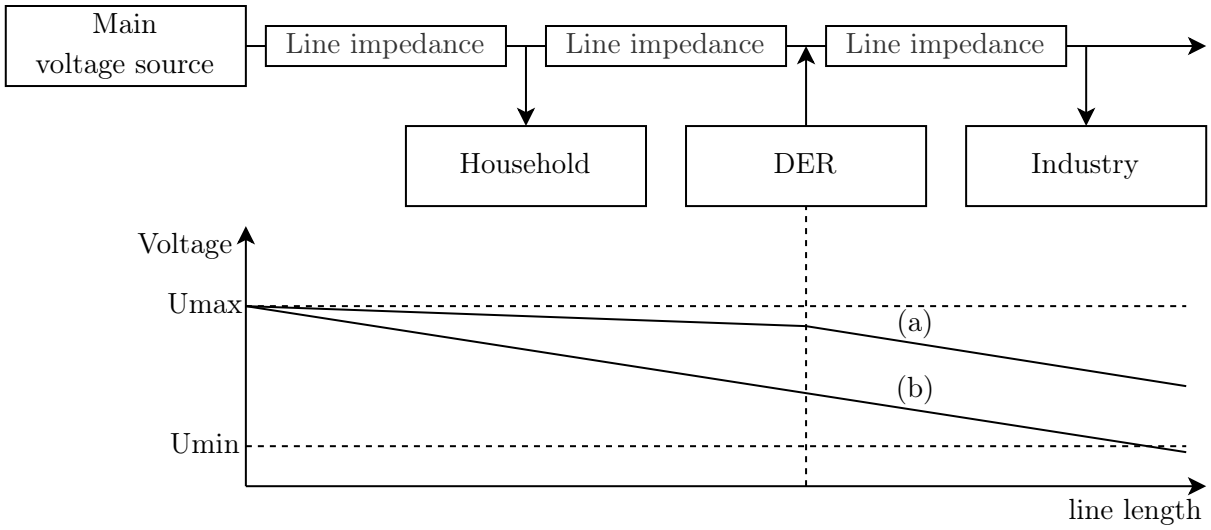

Figure 1: Basic interpretation of DER impact, (a) is with DER, (b) is without DER

The implementation of these functions can be divided into four layers and is based on methods used in [8]. In the first layer, P(U) and Q(U) characteristics will be implemented. While this layer focuses on voltage support, switching on or off loads, as indicated above, can be used to simulate variations in voltage levels. This will allow the characteristics to control the P and Q output. Before proceeding to the next layer, the current model has to be validated based on defined grid scenarios respecting both voltage events (switching loads) and different voltage levels (smooth voltage change) to make sure the characteristics are implemented correctly. Similar validation process has to be done between every layer. The second layer consists of a frequency support characteristic P(f). The third layer focuses on fault-ride-through capabilities of the DER. In this layer, time constants are becoming important while they define the maximum recovery time of e.g. voltage outage. The fourth layer makes sure the DER itself is protected against voltage and frequency deviations. These deviations have to be evaluated in the time domain to disconnect the DER when du/dt and df/dt are outside predefined levels [7]. Simulating in the continuous time domain requires a considerable amount of computing power and time. While this master's thesis only focuses on the magnitude and phase angle, the phasor simulation method can undoubtedly reduce simulation time to the point where real-time simulation is feasible [9]. For this reason, simulations will seem more realistic for the operator.

2 State of the art

2.1 Introduction

To make sure all work is a contribution for further research and not a rework of another project, it is necessary to know what already exists, how it works and why it does not suffice anymore for the current situation. Most of the voltage support is provided by OLTCs. In Belgium, once or more per year (depending on the necessity) the tap stand is changed to meet voltage limits. This is done manually, but more automated solutions are being implemented. These voltage control methods are discussed in the first subsection. Unfortunately, every method has its drawbacks for being 100 % effective. To provide extra support for OLTCs , or even fully replace them, DERs based on inverters can be used. Both active power (P) and reactive power (Q) compensation methods can be implemented to support voltage and frequency deviations. Instead of using inverters, an alternative approach is to use DSM. The general requirements are higher and is dependent on the household participation grade. Nonetheless, this technique can be undoubtedly provide noticeable voltage support.

Figure 2 shows a schematic overview of the literature discussed above and its interconnections. The focus on photovoltaic (PV) inverters is due to

- being the most accessible in a domestic installation,
- requiring little to no maintenance,
- an even distribution across the grid.

A smart meter can provide the DSOs with important information regarding the voltage levels and effectiveness of PV support. Both LV and medium-voltage (MV) suffer from voltage issues and the broad applicability and fast reaction times of inverters are a surplus.

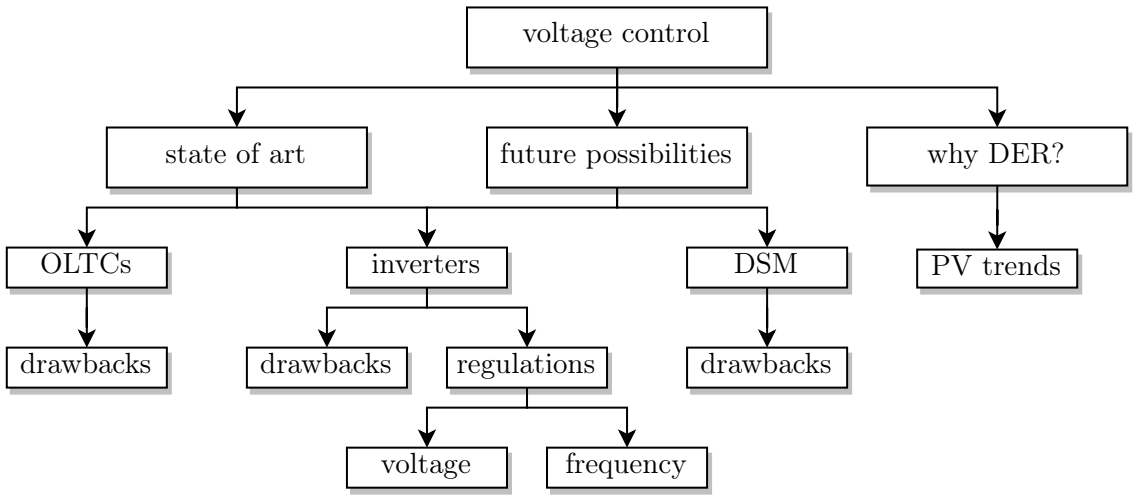

Figure 2: Overview of the state of art discussed in this chapter and future possibilities of grid control techniques

2.2 On-load tap changer

OLTCs are used by DSOs to change the voltage across the entire feeder [10]. This could be useful in situations as illustrated in Figure 3(b) because voltage levels as a function of distance are comparable on feeder a and b. In Figure 4(b) it is clearly visible that both feeders have a different voltage pattern and an OLTC would not suffice. Reasons for differences in voltage patterns can be a variation in number of households, industries and/or DERs connected to a specific feeder. Load flow simulations show that DERs affect the performance of OLTCs equipped with voltage compensation in a negative way [11]. Please note that the two feeders illustrated in both figures can also be two phases from a three-phase system. The variation in 4(b) arises when the power usage is not evenly distributed between the three phases [1].

Two terms, dynamic voltage control need (DVCN) (Figure 3(a)) and local voltage control need (LVCN) (Figure 4(a)), are introduced to better understand the influence and drawbacks of OLTCs. DVCN is used when the voltage level of all feeders coming from the same transformer need to or can be changed. LVCN indicates the need of changing the voltage level in a specific feeder [1].

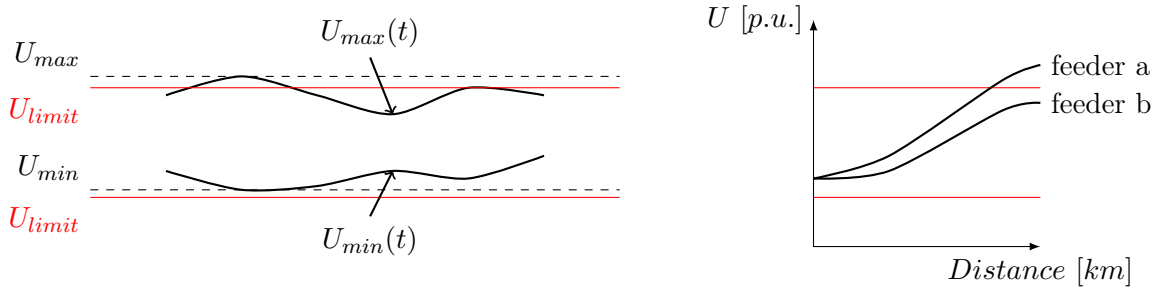

Figure 3: DVCN: (a) definition and (b) example [1, p. 19]

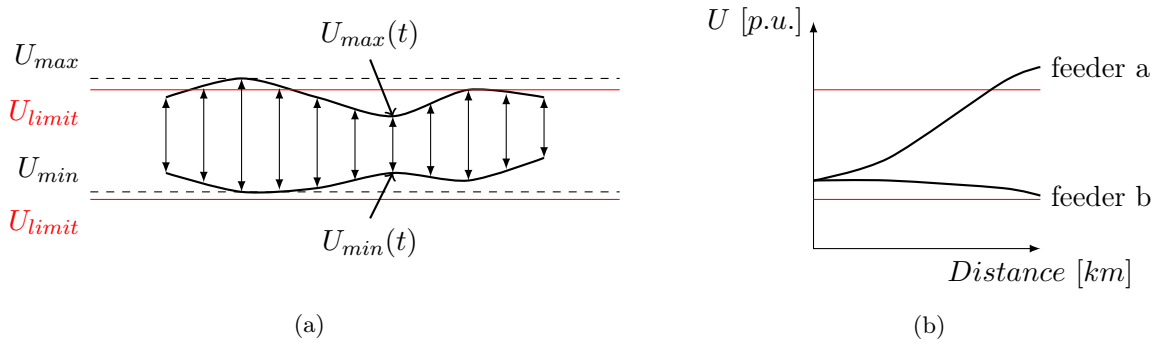

Figure 4: LVCN: (a) definition and (b) example [1, p. 19]

Based on Figures 3 and 4 it can be concluded that LVCN is an issue which cannot be solved by OLTCs. Accordingly, the control methods discussed below are based on feeders with a DVCN.

2.2.1 Voltage control by secondary transformer voltage

The first option, as shown in Figure 5, is to control the OLTC by measuring the voltage directly at the secondary winding of the transformer. This will compensate the voltage variations caused by the MV grid but it does not take the voltage drop caused by the loads and impedance Z into account. As a result, voltage problems may still occur at the end of the feeder. From this figure we can also deduce that more feeders are connected to one transformer (which is a normal situation). By changing the tap stand, voltage problems may be solved in the upper feeder, but even more voltage problems can occur in the lower feeder. To clarify, the upper feeder might have an undervoltage problem while the lower feeder has an overvoltage problem. By changing the tap stand in favor of the upper feeder, the lower feeder will have more overvoltage problems.

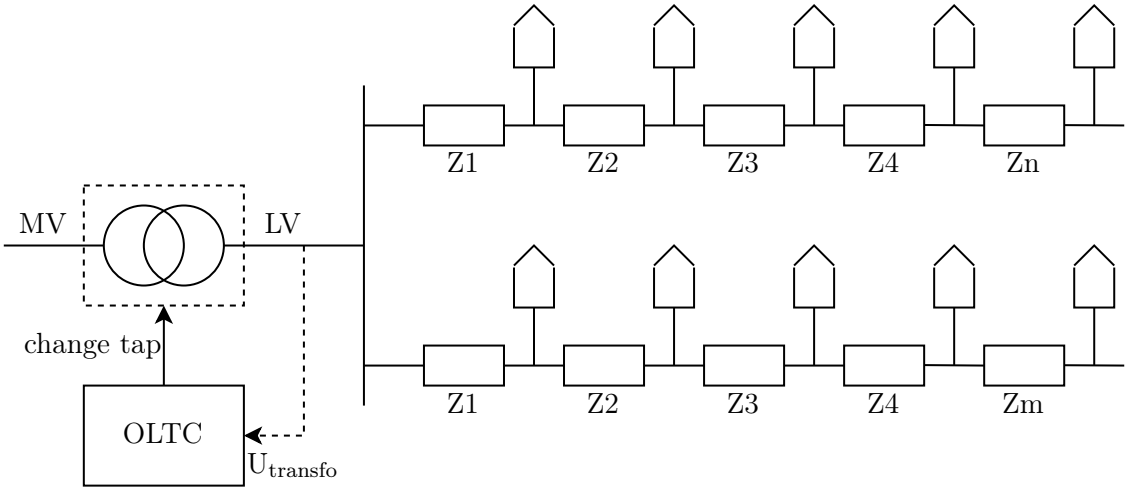

Figure 5: OLTC controlled by transformer voltage [10]

2.2.2 Voltage control by feeder end voltage

The second option is designed to solve the first option's drawbacks. As shown in Figure 6, voltage is measured at the end of the feeder, which makes sure minimum voltage level is maintained for every user. However, the voltage level at the secondary winding of the transformer is still limited to the maximum voltage allowed on the feeder. For long feeders or feeders with high power usage, voltage problems may still occur (see Figure 1b). Unfortunately, this technique poses also other challenges:

- the voltage in the upper feeder is still not controlled;
- the need for Power Line Communication or other communication techniques[1];
- the possibility of hacking into this communication line will have tremendous consequences.

[1]Other techniques (except wireless) will need extra communication cables

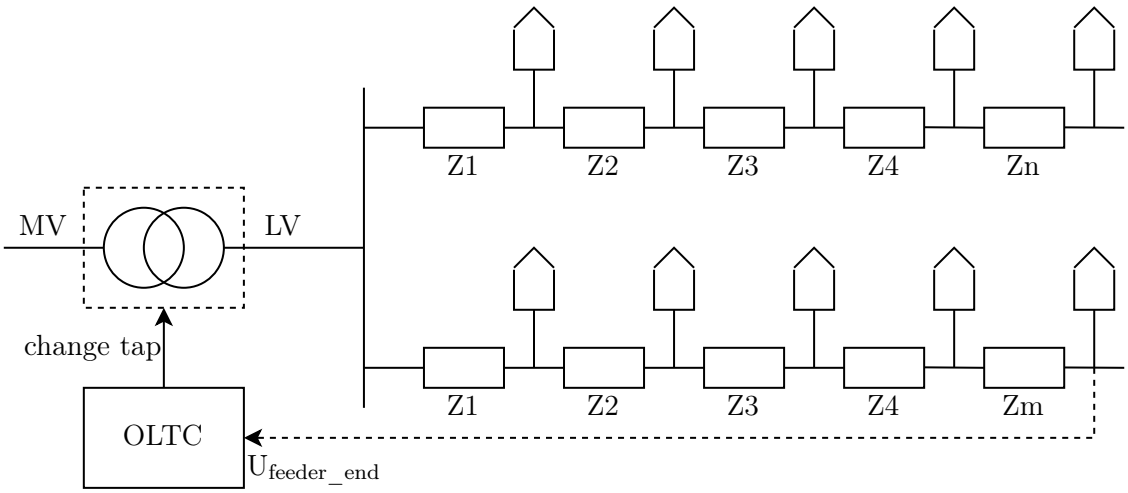

Figure 6: OLTC controlled by feeder end [10]

According to [12], using remote voltage measurement values from all the POCs can fully remediate the overvoltage violations via P control and decrease the voltage unbalances considerably via Q management. An example of the setup is shown in Figure 7 Unfortunately, the same challenges as in Figure 6 are present.

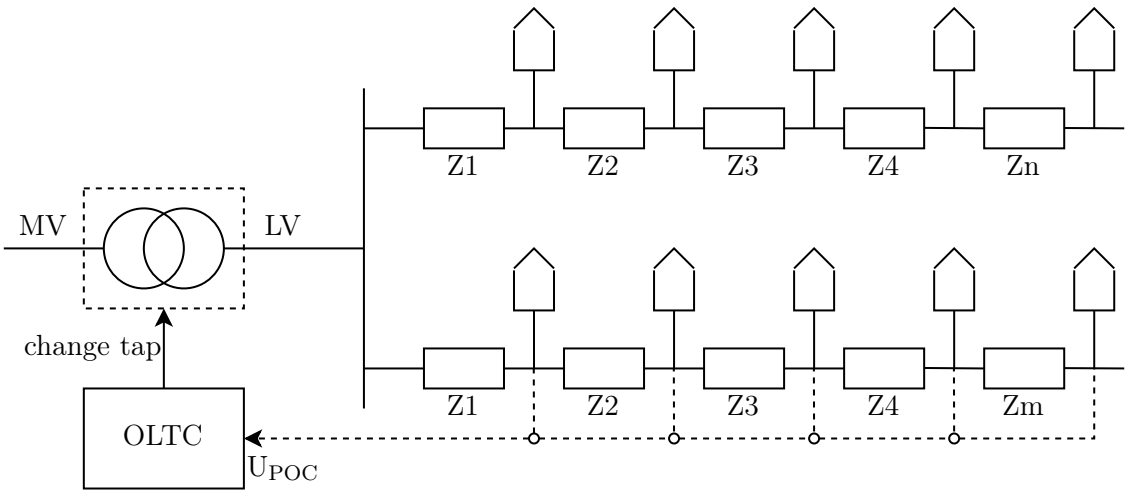

Figure 7: OLTC controlled by evaluating all POC voltage levels [12, p. 3]

2.2.3 Voltage control based on estimate

The method shown in Figure 8 estimates the feeder end voltage based on the voltage and power of the secondary transformer winding. A model of the correlation between voltage and power is implemented. This avoids the use of Power Line Communication and the mentioned possible communication issues. Despite this, voltage control based on an estimation brings in other challenges. In case the middle house has a PV installation, voltage limitations may still be exceeded at that POC. Also, the voltage level in the upper feeder is still dependent on the same tap stand of the bottom feeder.

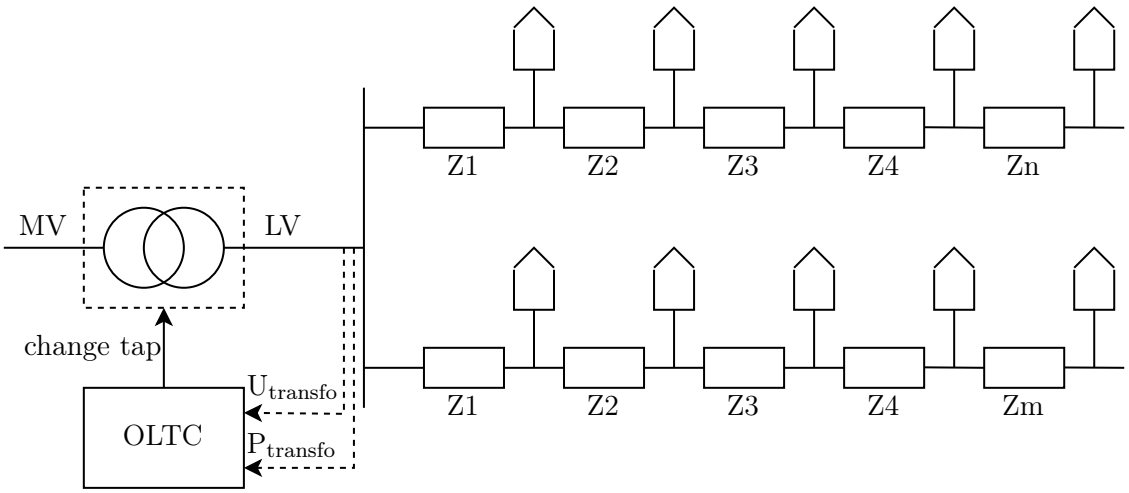

Figure 8: OLTC controlled by estimate [10]

None of the above techniques can provide a method that works for all of the possible scenarios. There is a need for extra support methods which are not reliant on OLTCs. One of those methods is the use of DERs based on inverters.

2.3 Inverters

As briefly mentioned above, the integration of DERs will result in an increased voltage at the point of connection. Due to fluctuating injection of power (solar and wind power is not constant) the need for automated solutions is growing, which implies that (even automated) OLTCs are not sufficient anymore. Using these DERs to compensate for low or high voltage is one of the most commonly discussed methods [1], [3], [13].

Three main types of an inverter, a string inverter, a micro-inverter and a central inverter, exist [14], [15]. A string inverter is based on solar panels connected in series. When one PV panel is shaded or malfunctions, the entire power output is limited by this one panel. A malfunctioning PV panel can be replaced, but shade caused by trees can often not be controlled by the owner. To overcome this, a micro-inverter can be installed instead. The PV panels are connected in parallel and therefore only the shaded or malfunctioning panels are limited in output power. The difference with a central inverter is the size. Central inverters are mainly used in industrial installations with typical power ranges from 100 kW to 1 MW [15]. The study in [14] also shows that micro-inverter systems present better performances both at shaded and not-shaded conditions. The main drawback of a micro-inverter is the higher cost. However, according to [16, p. 2885]

> the string inverter appears to have a lower per-watt capital cost when just the inverter is considered. However, the inverter represents only about 15 % of the entire PV system cost whereas the installation labor (...) cost accounts for 40 %, depending on the system configuration and inverter technology. These factors have made it difficult to perform a comparative cost study.

Figure 9 shows the different inputs needed for a controllable PV inverter to function as grid support. P is used to determine Q output (Q(P) → Q(U) → Q output). The Q mode determines the actual Q output. The PV inverters are used in combination with a storage system, which performs as a buffer for the grid and enables the system to absorb power when the upper voltage limit is exceeded.

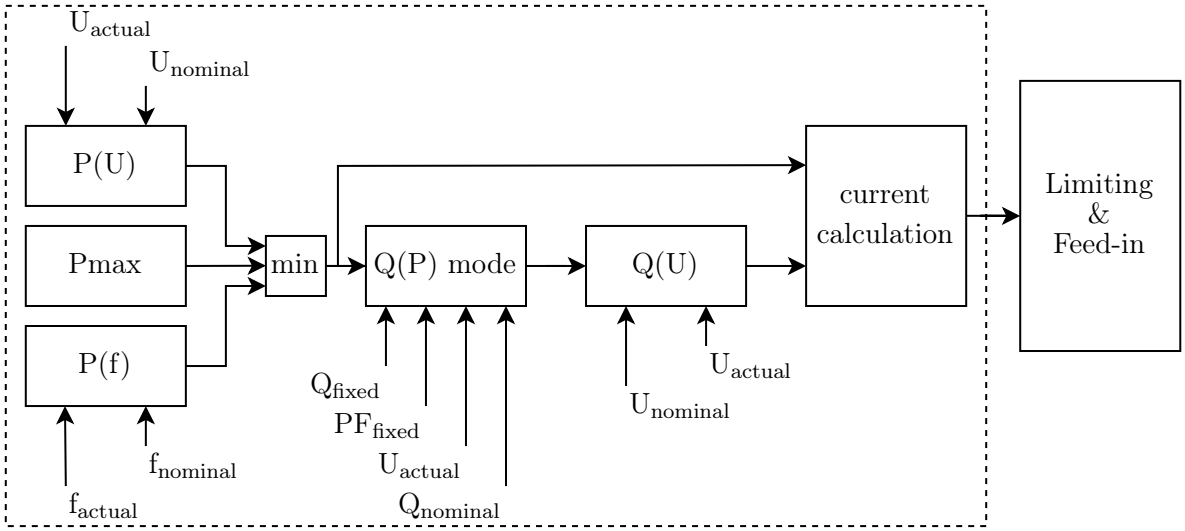

Figure 9: Grid support management of a controllable PV-inverter [2, p. 113]

The following functions are also known as advanced inverter functions and are discussed in [1], [17]. The setpoints can differ according to the local requirements.

2.3.1 Active power compensation

Figure 10 shows the possibility and settings of the inverter to absorb P when there is overvoltage in the LV grid. First, it should be noted that this is only possible if a storage system is present to absorb P. If not, the inverter can reduce its P output and, if necessary, be disconnected from the grid. This will only happen in extreme situations. Also, being disconnected from the grid will cause a loss of income for the energy producer, so this should be avoided as much as possible. Second, this compensation is only available until the storage system is fully charged or until a threshold charge is reached. The rated active power P_r is used as a baseline value to determine the absorbing capabilities of the inverter.

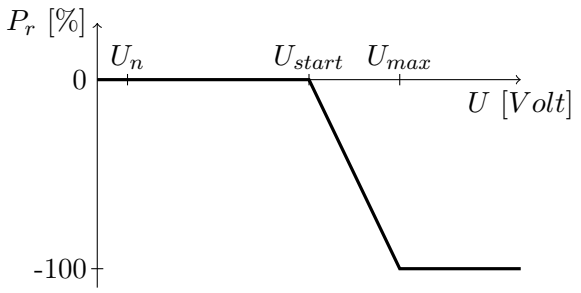

Figure 10: P(U) characteristic for overvoltage mitigation with storage system [1, p. 15], [17, p. 3]

2.3.2 Reactive power compensation

In MV or LV grids where the reactance X is important, Q(U) compensation is used. In order to alleviate a voltage drop caused by a grid event, the inverter needs to provide a certain amount of Q to the grid, as illustrated in Figure 11 [13], [18]. A dead-band (DB) is introduced, which will make sure the inverter will not switch continuously between absorbing or delivering Q. It should be noted again that this is only possible if a storage system is present to absorb Q. $Q_{\max}$ can be calculated using different methods depicted in Figure 9.

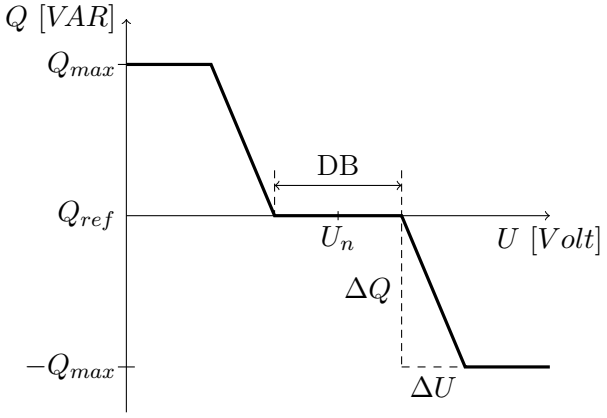

Figure 11: Q(U) characteristic for over- and undervoltage mitigation with storage system [1, p. 20], [17, p. 2]

Both P and Q compensation for overvoltage problems presume the presence of a storage system. While most of the (household) inverter-based DERs do not have a storage system, these characteristics are often replaced by reducing P and Q according to voltage levels.

2.3.3 DERMS and BESS

Two more solutions contained in [17], a DER management system (DERMS) and a battery energy storage system (BESS), are not further discussed in this thesis since the costs for those two methods are substantial. However

> it was found that a 7 MWh BESS would be required to provide an equivalent level of performance than about 29 MWh PV production curtailment through Volt-Watt control, for the month of June. When scaled for the full year, it was found that about 180 MWh would be curtailed under the same control method. [17, p. 5]

BESS definitely has potential, but the cost per MWh (which is now estimated at 1.5M USD) has to drop significantly. Also, this thesis assumes the possibility of changing function settings according to DSO request. This would require the use of DERMS. The study also shows that the Q(U) characteristic "is not an effective method to regulate voltage in distribution feeders with high (∼1) R/X ratio, as inverter ability to absorb VAR is limited" [17, p. 5].

2.4 Demand side management

DSM is seen as an important method to help mitigate the effects of:

- the increasing share of unpredictable renewable energy production,
- the increased electrical load due to fossil fuel powered equipment being replaced by electrical equipment,
- decreasing investments in directly-controllable (fossil fuel) plants.

Instead of limiting the output of an inverter, DSM focuses on limiting power usage in case of high load and does the opposite in case of high injection. Washing machines, hot water buffers and (in the future) electric vehicles may pose issues during peak hours. The purpose is to postpone the usage of these appliances. The amount of postponed power is represented as flexibility [4], [19].

2.4.1 Necessities

The requirements for successful DSM are the following:

- smart appliances,
- test families,
- flexibility,
- communication devices,
- energy storage.

Compared to using inverters, these requirements are more challenging. First, smart appliances are needed to control the power usage according to the voltage level at the POC, which was measured by a smart meter. These appliances consist of postponable appliances, such as dish-washers, washing machines and tumble dryers, and buffered appliances such as hot water buffers and electrical vehicles. Hot water buffers are considered to have the most influence on flexibility. Second, test families are equipped with a Home Energy Management System. One group was asked to alter their usage based on different energy tariffs during the day and the other group was equipped with an Automated Home Energy Management System. Smart appliances were turned on or off automatically but comfort, such as always being able to take a hot shower, was still provided. Appliances without smart capabilities were retrofitted with communication devices to ensure smart control.

Energy storage can play an important role in reducing injection peaks and high power demand. As shown in Figure 12, energy storage can i.a. be divided into electrical and thermal energy storage. Decentralized energy storage can be domestic battery packs which are used individually per household. On the other hand, centralized energy storage will cover for an entire district or even more. An example is the holiday park Terhills in Maasmechelen, Belgium. With the use of

Tesla batteries and a capacity of 18 MW, they can operate off-grid. A well known example in Belgium but neither based on electrical or thermal storage, is the water reservoir power plant in Coo, which has a capacity of 1164 MW [4], [20].

Cogeneration or also known as combined heat and power (CHP) generation is using the, normally lost, thermal energy from a power-generating module (PGM). An example of a micro-CHP, which can be used in households, is a Solenco Powerbox. It uses (the surplus of) electrical energy to produce hydrogen. In the process of producing hydrogen, a large amount of thermal energy is generated. Normally, this thermal energy is lost and as a result an efficiency of 25-35 % is reached. By storing the thermal energy in a hot water buffer, an efficiency of 95 % is viable [21].

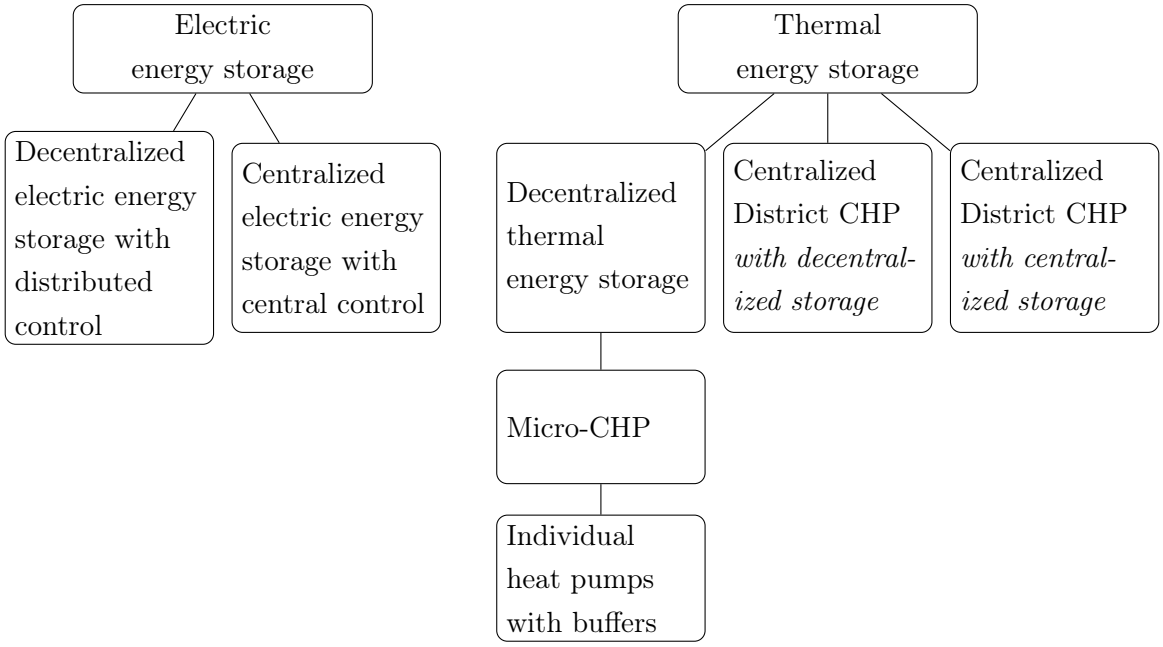

Figure 12: Electrical and thermal energy storage concepts [4, p. 26]

The basic layout of a Solenco powerbox is illustrated in Figure 13. The inputs consist of (the surplus of) electric energy and water for the thermal energy transfer. The inside consists of a power management system, a fuel cell (which can be compared to an electric battery) and a hot water buffer. The outputs are thermal energy, represented as hot water, and electric energy produced by the fuel cell.

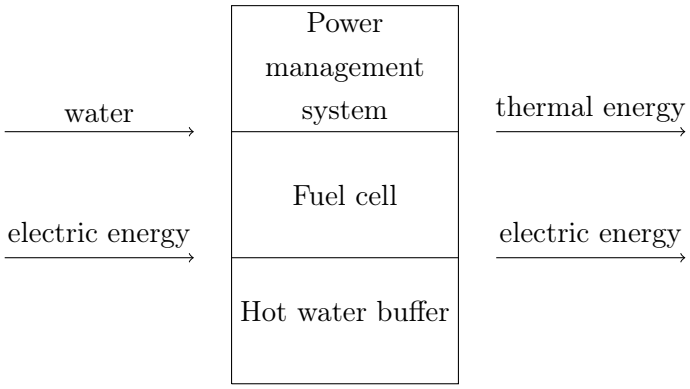

Figure 13: Micro-CHP with the use of hydrogen [21]

2.4.2 Flexibility

Figure 14 illustrates the flexibility potential caused by dishwashers, tumble dryers and washing machines. The color scale indicates in hours how long a power shift is possible. For example, in weekExtra there is only a few MW (in dark red) that can be delayed for 24 hours. Extra means the ability to turn on extra appliances in case of overvoltage while delay means the ability to postpone appliances in case of undervoltage. While weekExtra provides around 1000 MW flexibility at 20.00 h and weekDelay merely 200 MW, it becomes clear that the delay of power usage is in general more difficult to fulfill. This may be due to the fact that families did not provide all the available flexibility they can theoretically (or want to) deliver. On the other hand, flexibility to consume more power when needed is easier to find but often not necessary.

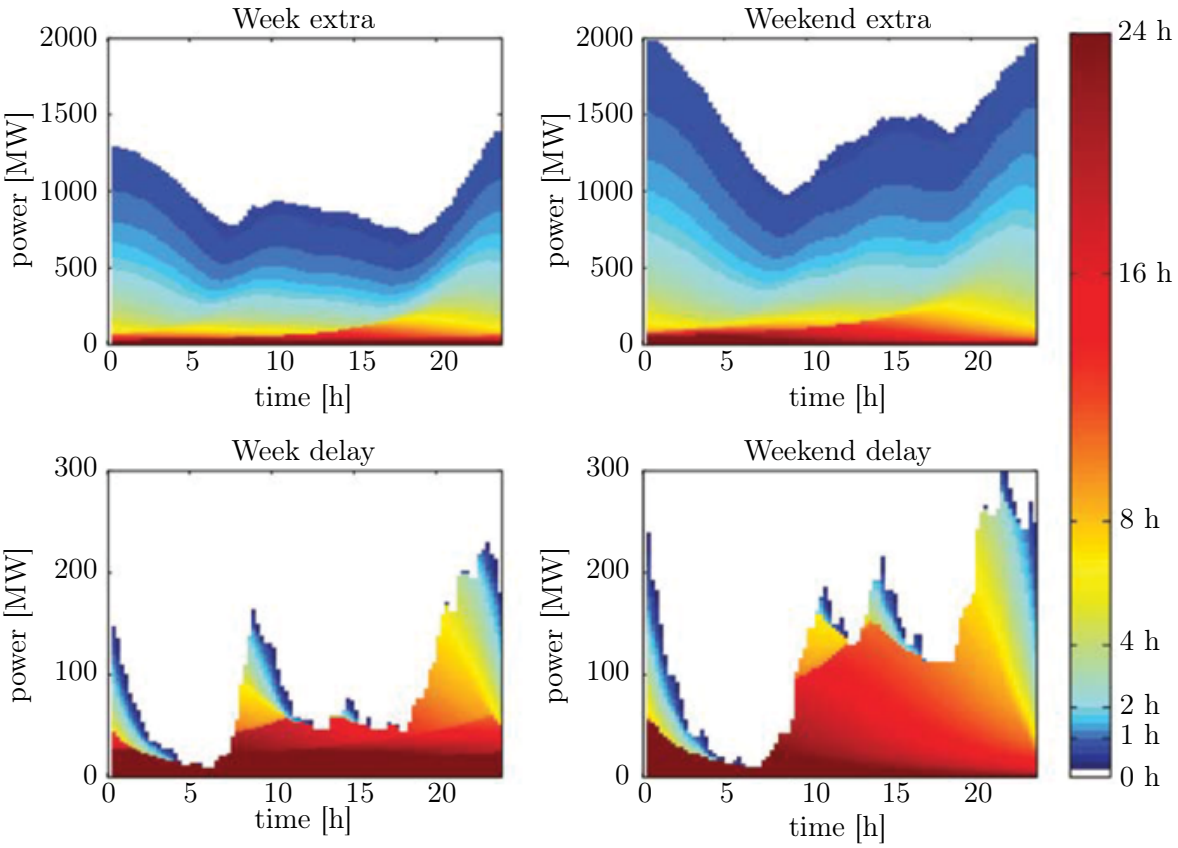

Figure 14: Flexibility potential [4, p. 80]

2.4.3 Black-out

Considering that 18 % of Flemish households heat their water using electricity (hot water buffers have the most impact as mentioned above), extrapolating this for the whole population of Belgium would provide 207 MW of delayed power usage. Taking into account the other appliances (washing machines, electric vehicles, etc.) adds up to 267.9 MW. Comparing these values to the 725 MW strategic reserve that Belgian Transmission System Operator (TSO) Elia has to create, it can be assumed that, even with a participation grade of 100 % of households with hot water buffers, the requirement will not be met [4], [22].

2.5 Trends in photovoltaic applications

PV installations are becoming more popular and are the major part of DER, which is also shown in the 2019 IEA PVPS report [5]. The exponential growth of installed PV capacity, as shown in Figure 15, is a first argument why these installations could impact the distribution grid, and also why they can and should be used as grid support.

PV contributes 2.9 % of the global electricity demand in 2018 [5]. One reason PV has not broken through, is the existing limit in Watt-peak (Wp) per module. This value is ranging between 145 Wp and 350 Wp, depending on its quality and size. It is important to note that this is a peak value and not a nominal value. In order to achieve this, it is necessary to have perfect conditions: a pitched and south-facing roof, no clouds, no trees or other shadows, et cetera. Another reason is due to the dependence on sunlight for generating power. Northern countries of the Europe will have less sunlight per day than southern countries. Southern countries also have higher temperatures which have a negative impact on the solar panel voltage level [23]. Multiple factors, as mentioned above, should be taken into account to determine if it is profitable, both economically and in terms of energy yield.

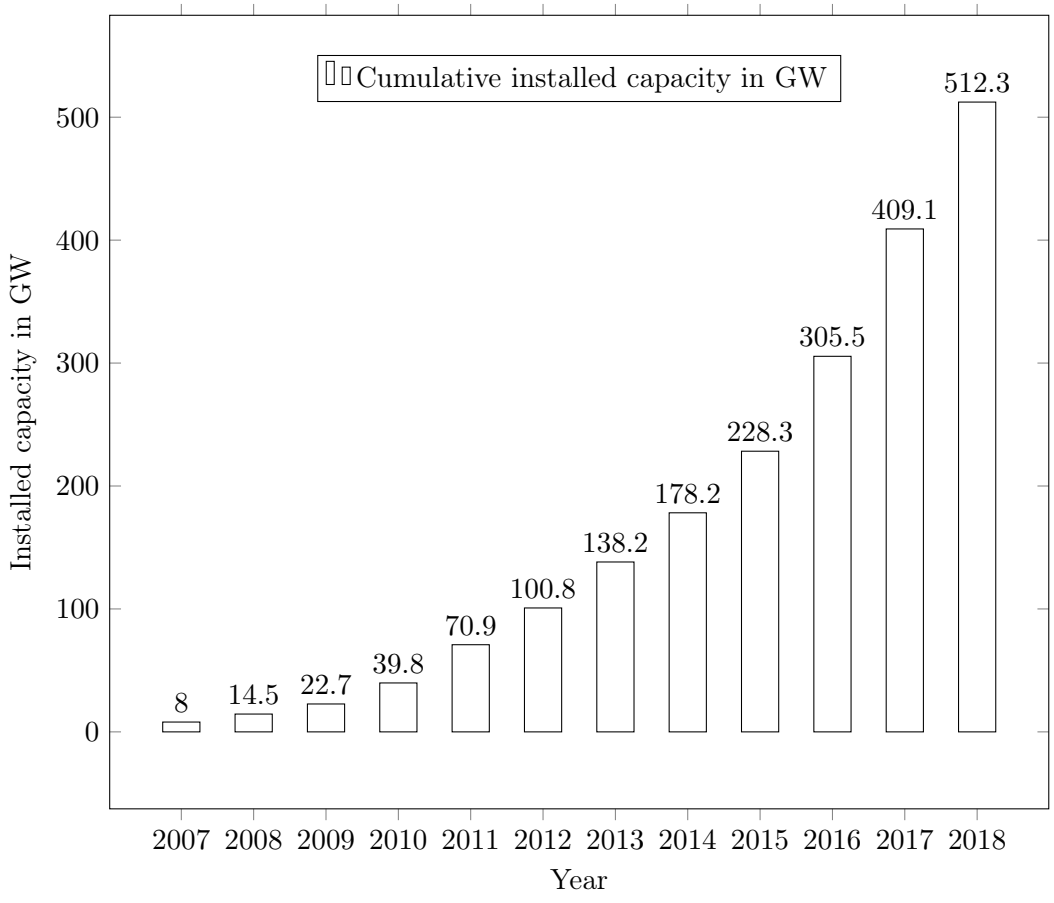

Figure 15: Exponential growth of cumulative installed PV capacity, worldwide [5, p. 11]

2.5.1 Comparison between Belgium and Czech Republic

As shown in Figure 16, the suitability [23] for PV panels, based on climate, is comparable between Belgium and Czech Republic. Therefore, a more detailed comparison shown in Table 1 can be made. Belgium has a higher electricity consumption and PV penetration. The lower percentage of PV penetration in Czech Republic is due to barely adding new capacity in 2018 [5]. A comparison with the European average is a difficult exercise since many variables, such as electricity consumption and inhabitants, differ. Therefore, it will not be a correct indicator.

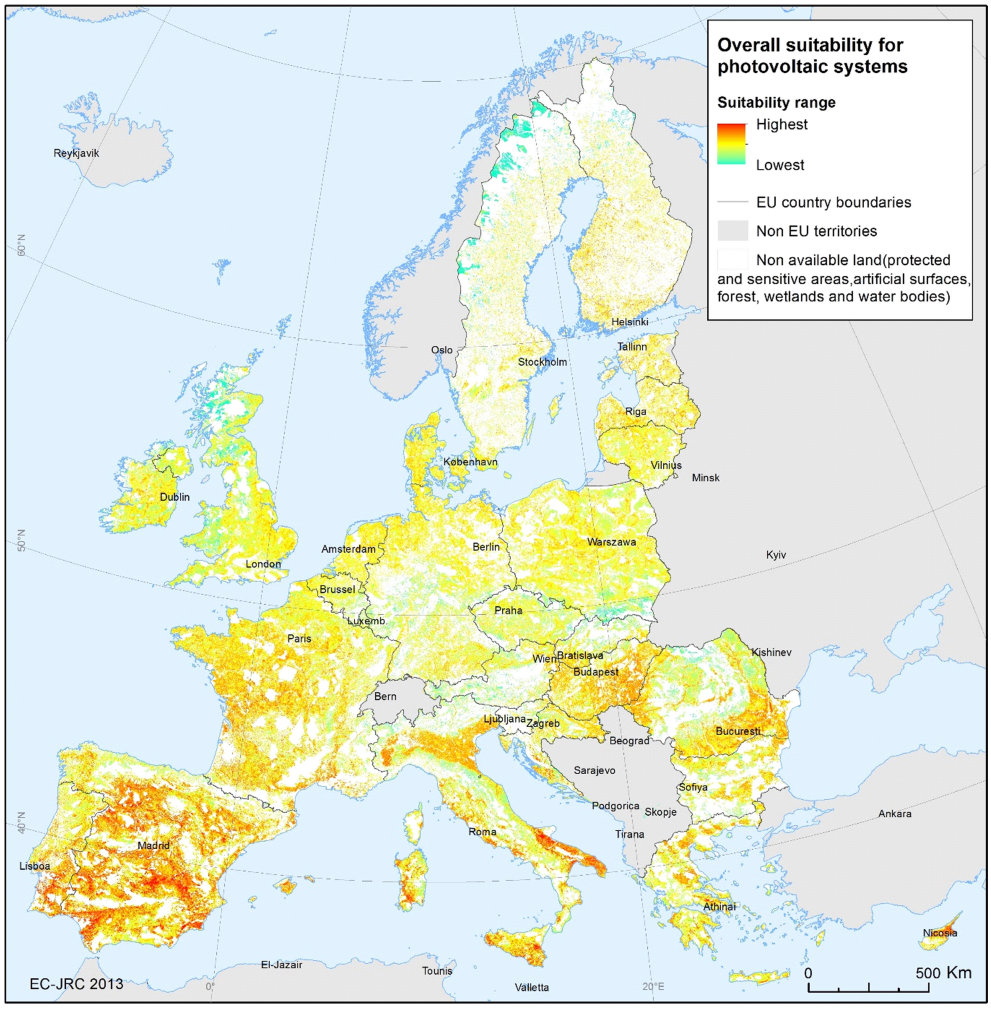

Figure 16: The suitability for (large scale) PV systems, based on weather conditions [23, p. 91]

Table 1: A comparison between Belgium and Czech Republic in 2018 [5]

	Belgium	**Czech Republic**	**unit**
Electricity consumption	87	67	TWh
Inhabitants	11	10.5	$Million$
Average yield	962	unknown	kWh/kW
Total installed capacity	4.3	2.2	GW_{DC}
PV penetration	4.3	3.6	$percent$
PV penetration per capita	380	≈ 210	$W/inhab$

2.5.2 Actions to stimulate photovoltaic

The most common method, as shown in Figure 17, is a feed-in tariff (64 %). This is a by-law structure to stimulate investments in renewable energy resources (RERs). Electricity produced by the PV system and injected into the grid is paid at a predefined price and guaranteed during a fixed period. This assumes that PV is mostly injecting power into the grid instead of self-consuming. Net metering[2] (14 %) allows consumers to use their generated electricity at a different time. This can be further divided between monthly and annual. Otherwise, a battery should be installed and this entails costs that make the purchase of a PV installation out of consideration. Direct subsidies (12 %) fulfills the top three.

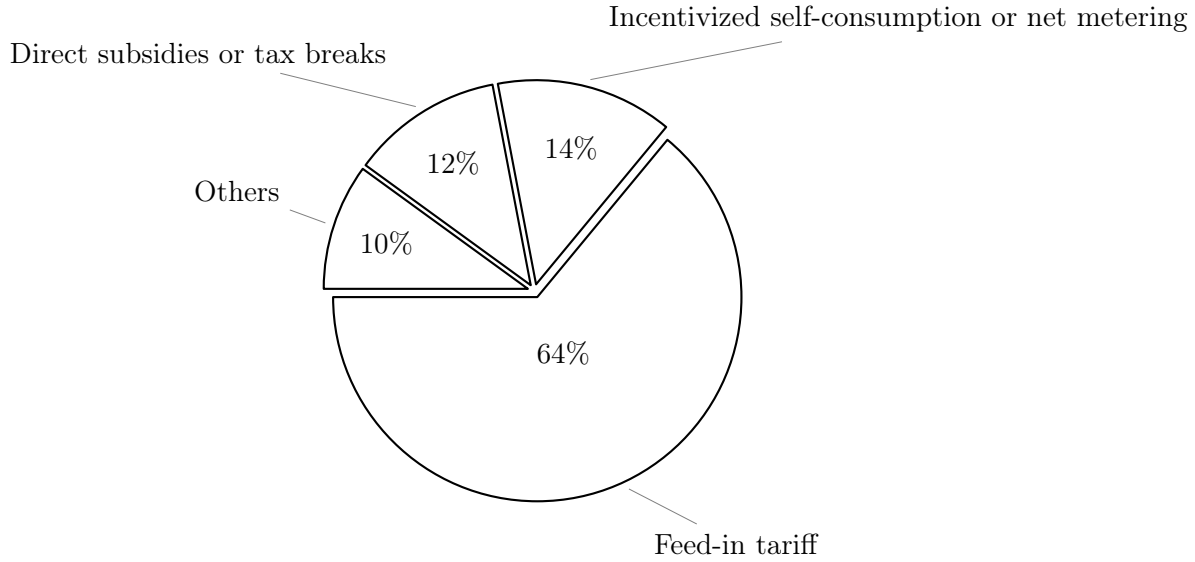

Figure 17: Main drivers of the distributed PV market in 2018 [5, p. 48]

2.5.3 Emissions

Worldwide, all the (power-consuming) sectors contribute to around 38 % of the energy-related CO_2 emissions. Increasing and stimulating PV production can significantly reduce these emissions, as 1 kWh produced by PV emits as low as 15g/kWh CO_2 compared to the global average of 475g/kWh CO_2. While merely 3 % of the electricity is generated by PV, it avoids around 4.5 % of the power sector emissions. This is due to countries with high carbon electricity generation, such as China and India, installing a great amount of PV [5].

[2]Belgium and Denmark are moving away from net metering [5].

3 European standards and regulations

This section summarizes the standards and regulations 2016/631 in [6] and the requirements for PGMs to be connected in parallel with distribution networks in [7] which are applicable for smaller and domestic (PV) installations. Establishing these standards and regulations take care of making a uniform decision across the interconnected European grid. Please note that all summarized values are valid for Continental Europe only.

3.1 Types of power-generating modules

The standards and regulations are divided according to their capacity. The bigger the PGM, the more impact it can have on frequency and voltage stability and the more requirements it has to meet. An overview of the types of PGMs is given in Table 2. This thesis will focus only on capacities less than 10 MW, so only type A and B is of importance and will be discussed further in this section. All of the standards, regulations and requirements for type A are also valid for type B and further types, unless stated otherwise. It is important to note that all inverters used for domestic PV installations should only meet the requirements for type A.

Table 2: Types of power generating modules [6, pp. 10-11]

Type	**Connection point**	**Capacity**
Type A	< 110 kV	0.8 kW $\leq$ capacity $<$ 1 MW
Type B	< 110 kV	1 MW $\leq$ capacity $<$ 10 MW
Type C	< 110 kV	10 MW $\leq$ capacity $<$ 50 MW
Type D	< 110 kV	$\geq$ 50 MW
	≥ 110 kV	n/a

3.2 Frequency stability

As shown in Table 3, PGMs should have ride-through capabilities when frequency is fluctuating. This is to prevent them from disconnecting and causing more issues. Since this table summarizes values for continental Europe, only a nominal frequency of 50 Hz is considered. Frequency deviations between 49.0 Hz and 51.0 Hz are most common so PGMs should be able to withstand those for an unlimited amount of time. Frequencies under 49.0 Hz are specified by the TSO with a minimum amount of time. The reason for not specifying this further in the standards is to enable TSOs to adjust PGMs in areas with high loads, thus areas with frequency drops. Table 3 only indicates the possibility of staying connected and not the possibility of delivering 100 % P.

Table 3: Frequency ranges and corresponding minimum time periods, type A and up [6, p. 14], [7, p. 22]

Frequency range	**Time period of operation**
47.5 Hz - 48.5 Hz	To be specified by each TSO, but not less than 30 minutes
48.5 Hz - 49.0 Hz	To be specified by each TSO, but not less than above period
49.0 Hz - 51.0 Hz	Unlimited
51.0 Hz - 51.5 Hz	30 minutes

3.2.1 Overfrequency

Figure 18 depicts a PGM operating mode which will result in P output reduction in response to a change in system frequency above a certain value. To calculate this slope, droop control s_2 is introduced. Note that the droop settings should be between 2 % and 12 %. Based on a given droop setting and Δf and P_{ref} measured at the inverter, a ΔP can be achieved:

$$s_2[\%] = 100 \times \frac{\mid \Delta f \mid - \mid \Delta f_1 \mid}{f_n} \times \frac{P_{ref}}{\mid \Delta P \mid} \tag{1}$$

This function should be interpreted as follows:

- f_n is the nominal frequency (usually 50 Hz or 60 Hz);
- Δf is the frequency deviation;
- Δf_1 is the frequency threshold (which has to be between 50.2 Hz and 50.5 Hz inclusive);
- P_{ref} is the P output at the moment Δf_1 is reached;
- ΔP is the change in P output from the PGM.

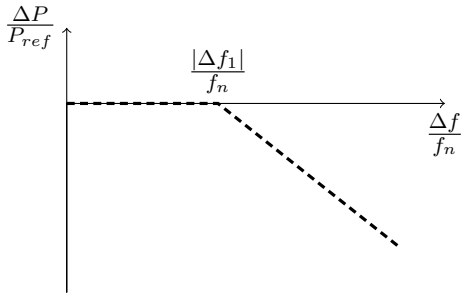

Figure 18: Droop control, type A and up [6, p. 16]

In this case, a DB is used to limit the inverter switching frequency. This DB should be smaller for inverters closer to the MV transformer so that inverters closer the the transformer respond quicker and deviations will not increase at the end of the line. This is also known as a location-based DB [1].

It is also possible to limit the PGM output after overfrequency until frequency drops below a certain value. This is also known as frequency value thresholding and is mentioned in [7] [3].

[3] see Figure 29

The benefits of droop control methods are given below:

- simple and easy implementation,
- reliability is high,
- high flexibility.

3.2.2 Underfrequency

When frequency is dropping, an allowable P reduction of the maximum capacity at 50 Hz is specified, according to the frequency level. As shown in Figure 19, a reduction rate of 2 $\%/Hz$ when frequency is below 49 Hz and a reduction rate of 10 $\%/Hz$ when frequency is below 49,5 Hz are applied.

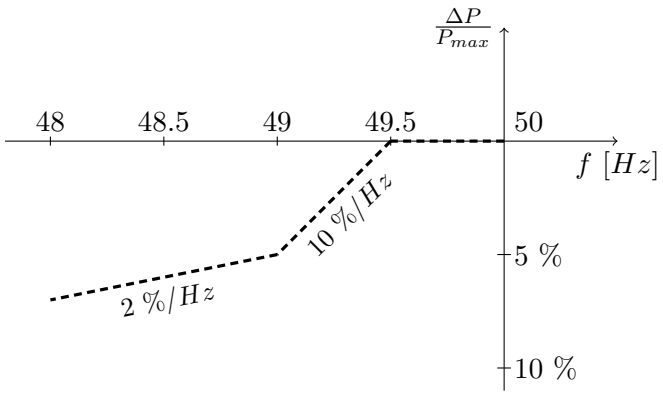

Figure 19: Maximum power capability reduction with falling frequency, type A and up [6, p. 17]

The actual P output depends on the amount of sunlight and clouds, also known as an availability factor. Therefore, the P_{max} on the y-axis indicates the available P instead of $P_{nominal}$. The available P is $P_{nominal}$ multiplied by the availability factor. The inverter needs to communicate the maximum power it can provide at a certain moment, i.e. by using a smart meter. Based on this value, the reduction can be calculated and applied.

This figure also indicates that the capability of increasing P output in case of under- frequency is not necessary for type A and type B. It is also important to take into consideration that this requirement for PV PGMs is limited since they are dependent on uncontrollable variables, i.e. the amount of sunlight.

3.3 Immunity to disturbances

While the immunity to disturbances is, among other things, dependent on the immunity of the power electronics of the inverter, simulating this is still possible by implementing virtual limits. Since this thesis focuses on developing a model for simulation purposes, this part will only give an overview of what the necessary capabilities are. How these functions are implemented in the simulation model is discussed in the next chapter.

3.3.1 ROCOF

Rate of change of frequency (ROCOF) is the frequency evaluated in the (continuous or discrete) time domain. df/dt is used to represent this value mathematically. According to [7], a synchronous PGM should withstand a minimum ROCOF of 1 Hz/s. This is a design requirement to protect the hardware of the PGM rather than a modelling requirement. The frequency is evaluated in a 500 ms window to filter incorrect measurement peaks. A maximum ROCOF value is not further defined.

3.3.2 Undervoltage ride through

Figure 20 shows the necessary capability of the PGM to withstand power outage. As long as voltage levels at the POC remain above the voltage-time curve. Table 4 summarizes the time parameters which are often further defined by the relevant TSO. The exact parameters depend on the needs in specific feeders.

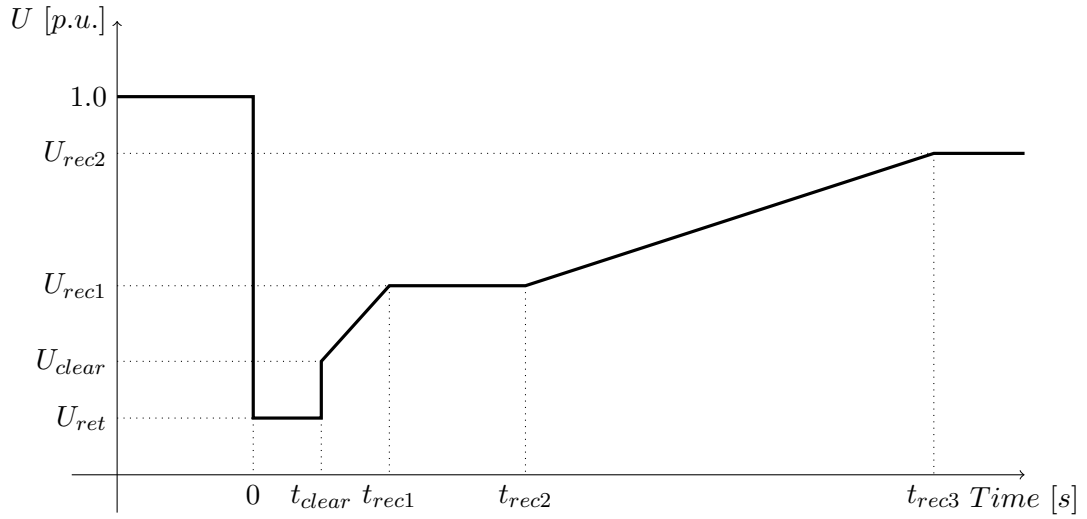

Figure 20: Fault-ride-through capabilities: voltage recovery, type B and up [6, p. 19], [7, p. 26]

Table 4: Undervoltage ride through capabilities, voltage and time parameters [6, p. 19]

Voltage parameters [p.u.]		**Time parameters [seconds]**	
U_{ret} :	0.05 - 0.15	t_{clear} :	0.14 - 0.15[4]
U_{clear} :	U_{ret} - 0.15	t_{rec1} :	t_{clear}
U_{rec1} :	U_{clear}	t_{rec2} :	t_{rec1}
U_{rec2} :	0.85	t_{rec3} :	1.5 - 3.0

[4] or 0.14 - 0.25 if system protection and secure operation so require

3.3.3 Overvoltage ride through

Overvoltage may be present for a limited amount of time. To prevent the PGM of disconnecting instantaneous when voltage levels are exceeded, overvoltage ride through should be implemented. As long as the voltage level at the point of connection is below the default requirement shown in Figure 21, the generating module should be capable of staying connected. This means that the PGM should be capable of staying connected for 60 seconds in total when the voltage level is between 1.10 - 1.25 p.u. [5]

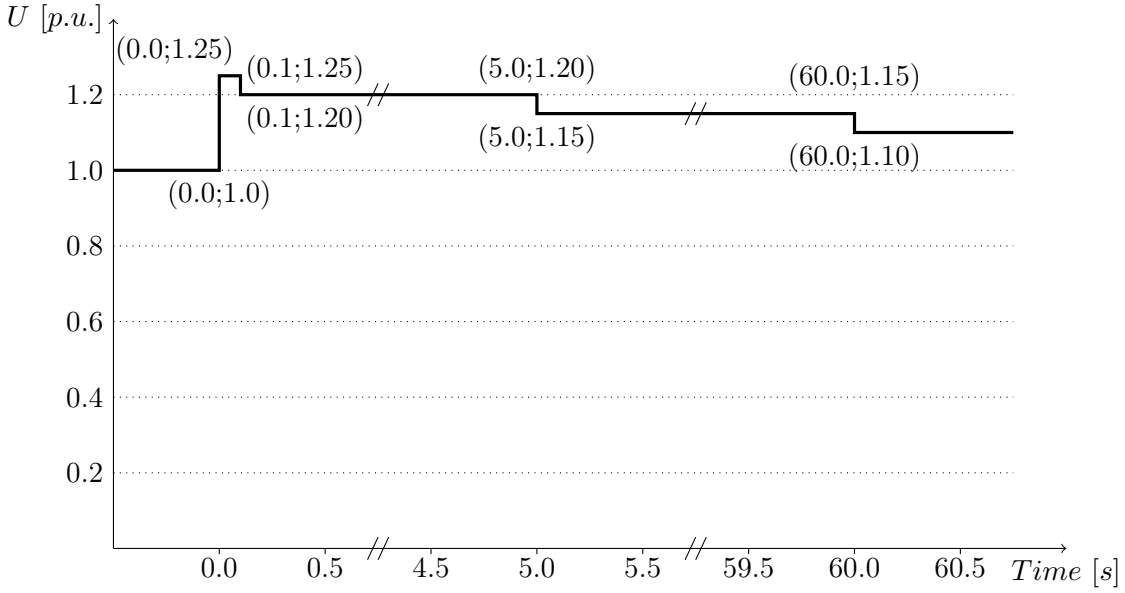

Figure 21: Overvoltage ride through capabilities [7, p. 27]

3.4 Reactive power capability

Figure 22 illustrates the Q capabilities depending on the maximum Q, known as design active power P_D. It is expected that the maximum amount of Q provided by the PGM is limited to 33 % P_D (with an absolute maximum of 48.4 %) when the available P[6] is above 20 % P_D. There may be exceptions provided by the relevant DSO that require a higher percentage of Q provided, in case there are feeders with high loads.

[5] 0.9 - 1.10 p.u. is the minimum requirement for staying connected for an unlimited amount of time

[6] $P_{nominal}$ multiplied by an availability factor, depending on the amount of sunlight for PV inverters, et cetera

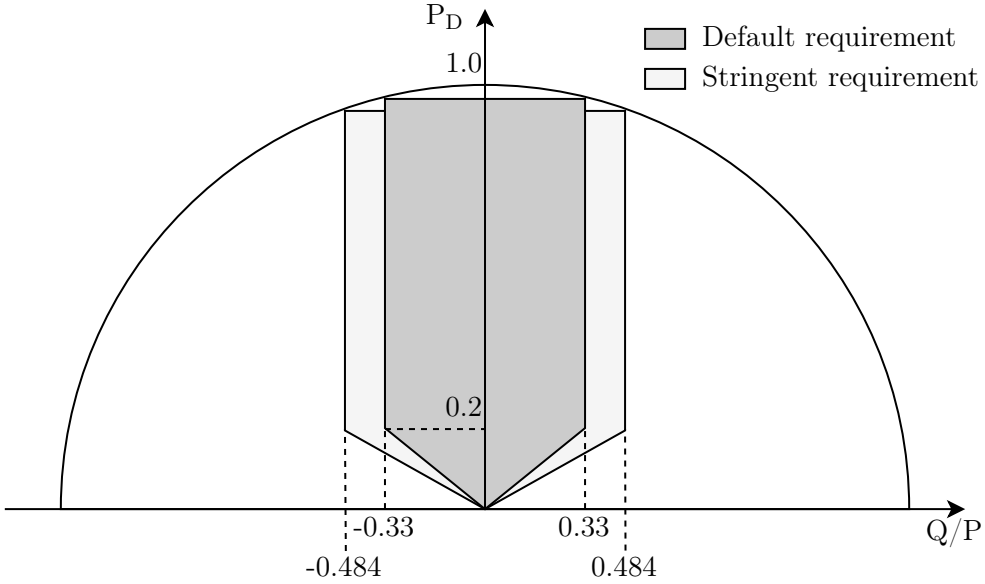

Figure 22: Default and stringent Q capability [7, p. 33]

4 Validation and implementation using MATLAB/Simulink

4.1 Introduction

The model is based on an existing model developed in PSCAD. Most of the functions and variables have the same value, which makes a comparison easy. Before designing a model, the general outlines are summarized in a flowchart. An equivalent grid model is designed using standard (adjustable) parameters.

The main difference between the PSCAD and the Simulink model is the solver. The PSCAD model uses a continuous solver which requires a considerable amount of computing power and time, while the Simulink model only focuses on magnitude and angle of output signals, better known as the phasor simulation method. For this reason, Simulink is chosen for developing the simulation model. This can undoubtedly reduce simulation time to the point where real-time simulation is feasible [9].

For better understanding, Simulink displays a color code which indicates the different sample times, summarized in Table 5. Measurements, such as voltage and current, output a continuous signal. The output of a discrete time transfer function outputs (in this case) a discrete signal with a sample time of 0.02s. Voltage and frequency step inputs, to simulate grid events, are sampled every 2 seconds and are indicated in green. Constant values, such as measurement errors, are pink and in case a subsystem or function has a combination of the above inputs, it is indicated as a yellow signal. This color code is used in all the Simulink screen captures.

Table 5: Color legend according to Simulink sample times

Color	Indication
black	continuous
red	0.02 s
green	2 s
pink	constant
yellow	multirate

4.2 Flowchart

The method, specific functions and necessary input values are illustrated in the Figure 23. The color code in Figure 23, clarified in the figure itself, is used to make clear where the inputs originate from. The DSO settings are, for simulation purposes, also part of the user settings. On the other hand, Figure 24 is color-coded using Table 5 since this is a screen capture from Simulink.

The user settings in Figure 23 can be linked to the edit boxes with red text description in Figure 24.

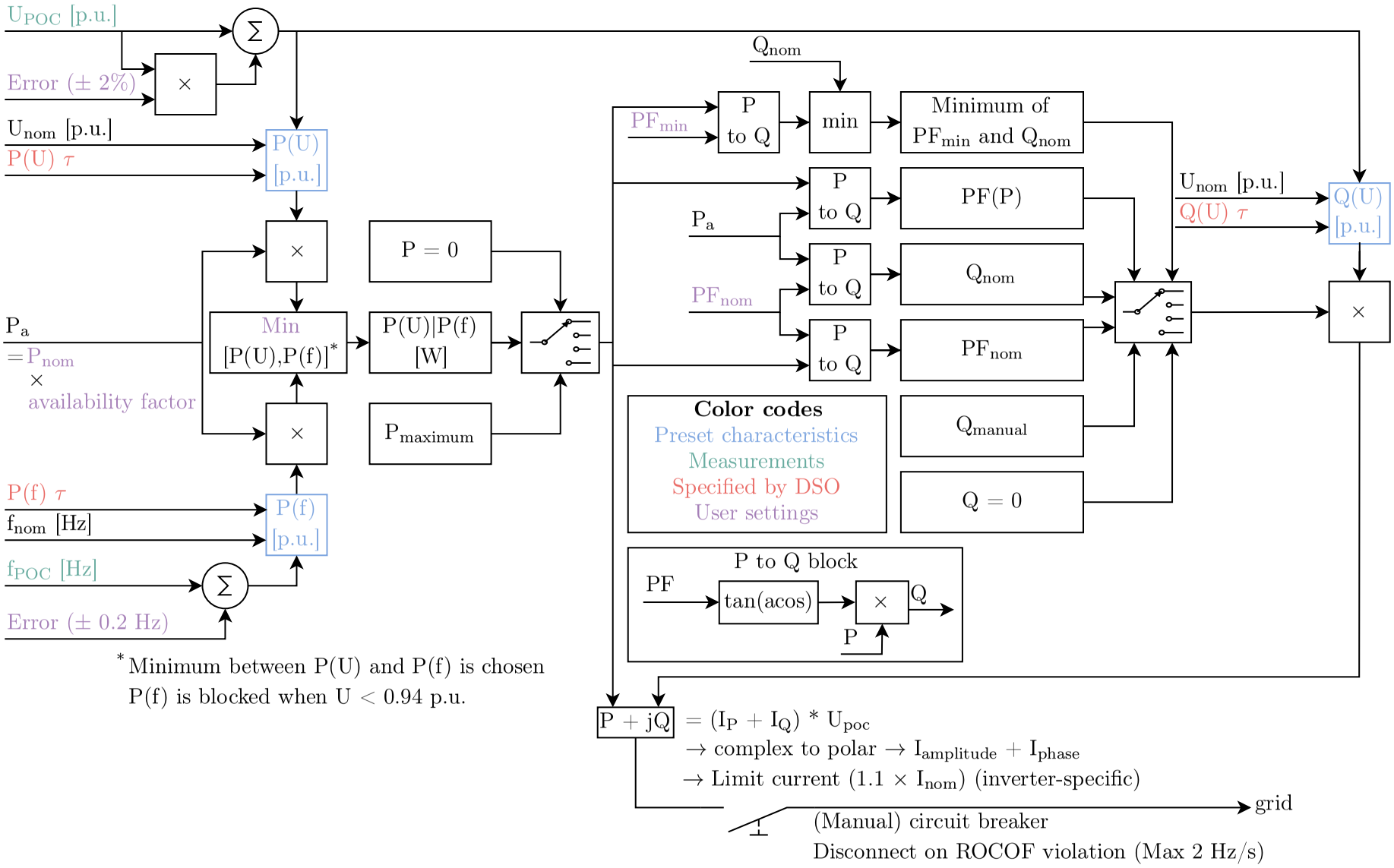

Figure 23: Extended flowchart with necessary inputs and calculations

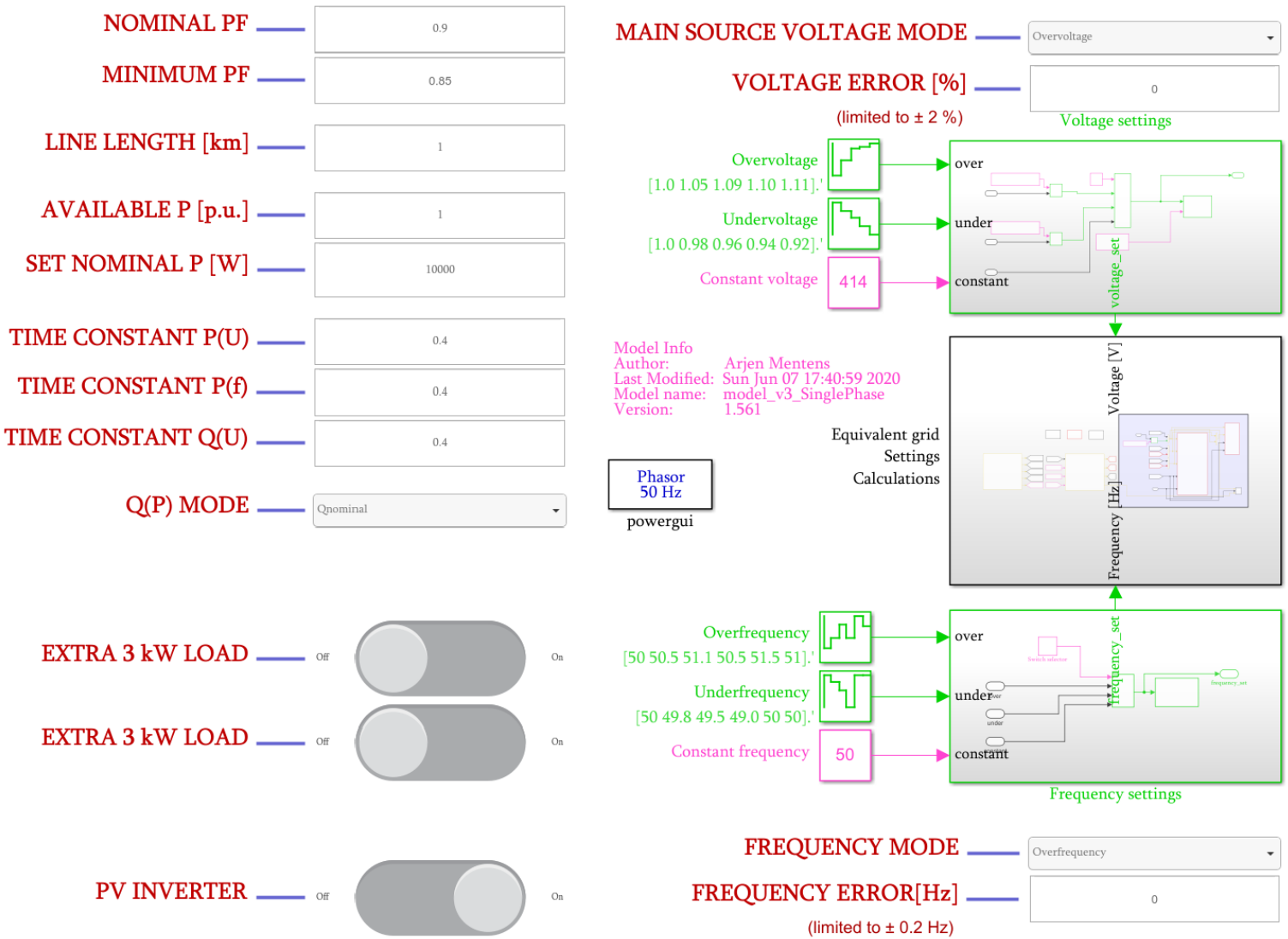

Figure 24: An overview of the control panel where the user can change inputs and settings

4.3 Equivalent grid model

The equivalent grid model, as illustrated in Figure 25, can be found in the 'calculations' subsystem in Figure 24. It is used as a realistic representation of a grid. Since the voltage source block is ideal[7], which indicates no losses, a source inductance is added to compensate for the short-circuit impedance of the second transformer winding. The line impedance is calculated based on the line length, with a resistance of 0.38 Ω per km and an inductance of 0.72 mH per km. While this model focuses on simulating voltage deviations by setting the source main voltage, only two main loads of 9.2 kW and two additional loads of 3 kW, which can be switched on to simulate high load situations, are used. A further segmentation of loads is not necessary, as this would make it difficult to simulate specific situations where only the voltage level is of importance.

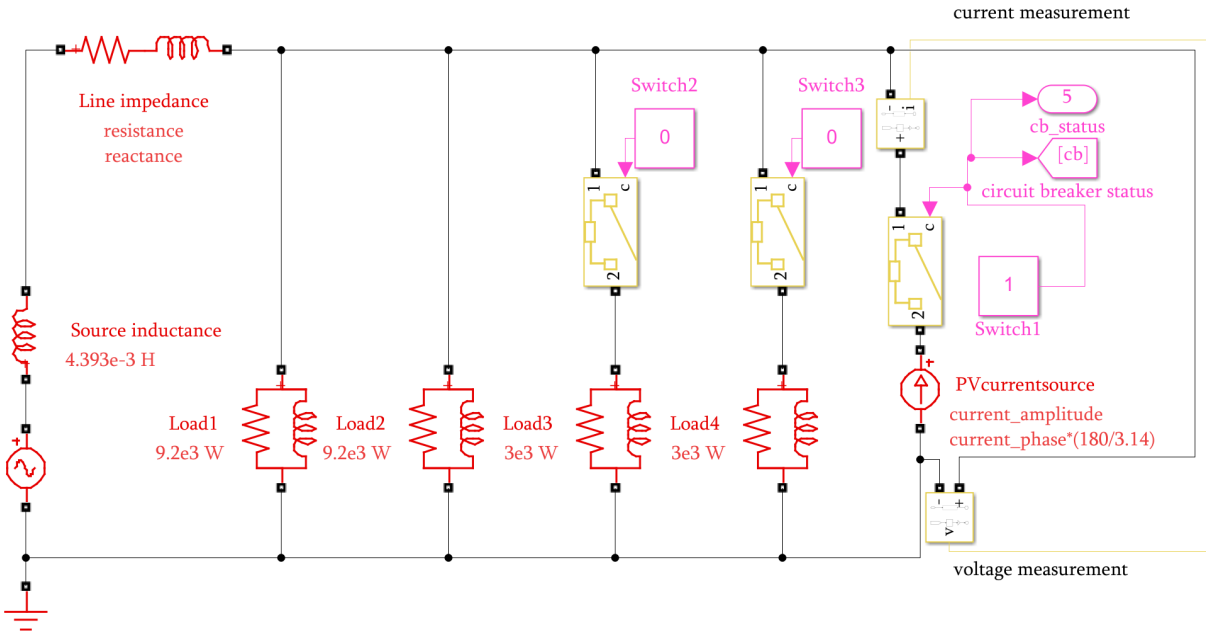

Figure 25: Equivalent single phase grid model

Simulink provides many useful standard blocks. Simple characteristics, such as P(U), Q(P) and Q(U) curves are implemented using 1-D lookup tables. The P(f) characteristic, implemented in layer 2, requires extra functionalities. More complex functions are therefore implemented using (a combination of 1-D lookup tables and MATLAB functions.

[7] this is the standard setting in Simulink

4.4 P(U) characteristic

As depicted in Figure 23 above, it is necessary to calculate P(U) and Q(U) to calculate $I_{amplitude}$ and I_{phase}. P is calculated by using a P(U) characteristic shown in Figure 26. The actual implementation is shown in Figure 27. The voltage [p.u.] values used for limiting P can differ according to DSO requirements. In this case, the same values as an existing PSCAD model are used, which makes it easier to compare and validate the model.

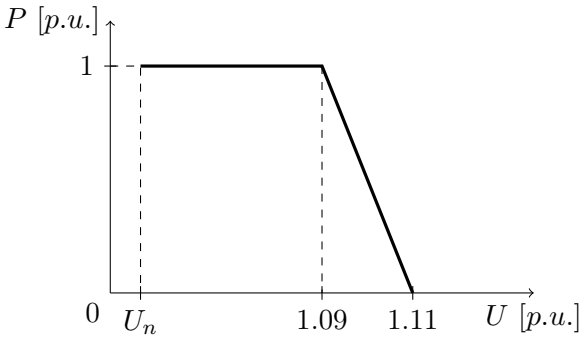

Figure 26: P(U) characteristic

While most regulations are based on p.u. values, this model also uses the voltage p.u. as an input for the P(U) characteristic. The implementation also requires a limit in output to prevent values lower than 0 and higher than 1. After this, the P(U) characteristic output is multiplied by the available P [8]. The availability factor can be used by the operator to limit the nominal power output caused by shadow, lack of sunlight, et cetera.

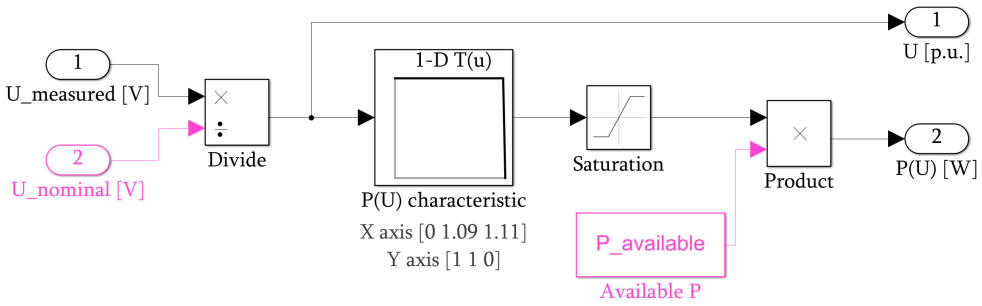

Figure 27: P(U) characteristic implemented in the model

[8] $P_{nominal}$ multiplied by an availability factor, depending on uncontrollable variables, e.g. sunlight

4.5 P(f) characteristic

DERs can also have an impact on frequency levels[9]. To compensate this change in frequency level, the power output can also be adapted if over- or underfrequency is present. Type A and type B PGMs should only provide support for overfrequency. The P(f) characteristic, shown in Figure 28, uses a value threshold to maintain 0.6 p.u. P output when frequency reaches 51.1 Hz. To prevent frequency levels from rising too fast again when frequency drops (P output will also rise again), the P output is limited to 0.6 p.u. until frequency drops below 50.1 Hz. This method is described in [7].

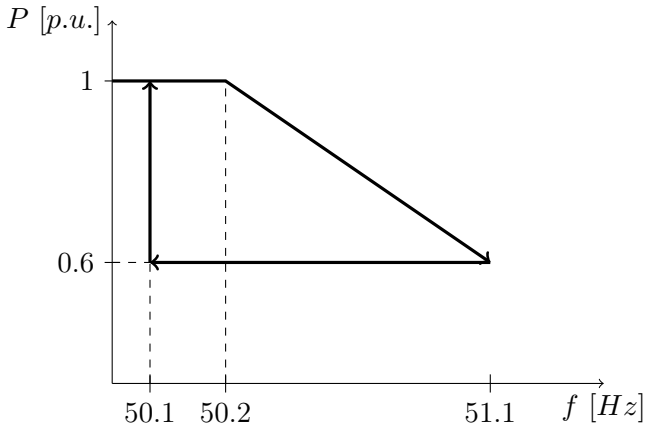

Figure 28: P(f) characteristic [7, p. 29]

A major drawback of using the phasor method is that a fixed frequency is used. The exact impact on frequency levels can therefore not be evaluated, but it can be manually adjusted to activate the P(f) characteristic.

The implementation in the model, shown in Figure 29 is more complicated. A value threshold cannot be added using a 1-D lookup table. Therefore, the threshold is programmed using a MATLAB function, shown in Figure 30. If the frequency reaches a value of 51.1 Hz, a boolean 'threshold' is set. If frequency is 50.1 Hz or lower, the boolean is reset. This boolean is used to overwrite the P(f) characteristic output if frequency is dropping from 51.1 Hz to 50.1 Hz.

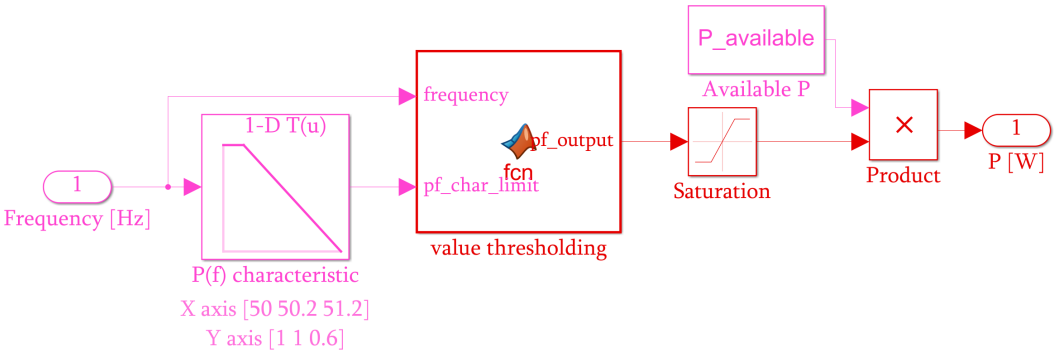

Figure 29: P(f) characteristic implemented in model

[9]A single DER will not have a visual impact, but adding them all together, will

```
function pf_output = fcn(frequency, pf_char_limit)
coder.extrinsic('get_param'), coder.extrinsic('assignin')
persistent temp, persistent threshold
if isempty(temp)
    temp = 0; threshold = false;
end
mdlWks = get_param('model_v3_SinglePhase','ModelWorkspace');
if frequency >= 51.1
    assignin(mdlWks,'threshold',true);
elseif threshold == true && frequency <= 50.1
    assignin(mdlWks,'threshold',false);
end
if threshold == true
    temp = 0.6;
elseif threshold == false
    temp = pf_char_limit;
end
pf_output = temp;
```

Figure 30: Frequency value thresholding for limiting the P output during overfrequency

4.6 Q(P) modes

The output of the P(U) or P(f) characteristic is used as an input for calculating Q(P). This can be calculated using different user-specific Q modes. The following paragraphs explain all the modes shown in Figure 31. The switch selector is connected to a knob, so that operators can easily switch between the preferred mode.

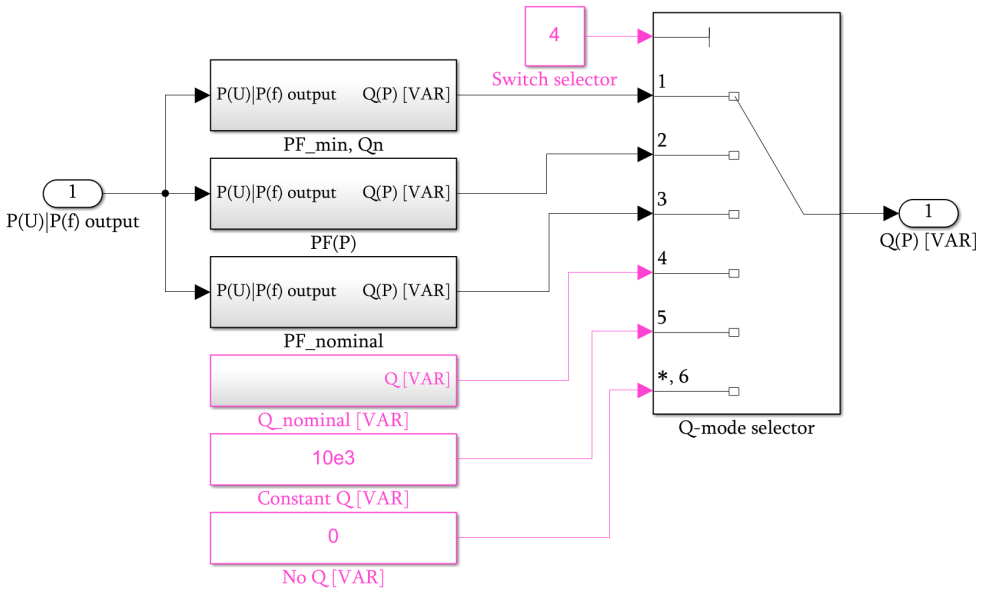

Figure 31: Overview of the Q(P) modes discussed in the following subsections

4.6.1 Q(P) mode 1

The first Q mode, shown in Figure 32, outputs the minimum value between $Q_{nominal}$ and Q_{PFmin}. The minimum power factor (PF) in the model is 0.85 but can be changed by the user. Note that the P input for both subsystems is different. For calculating $Q_{nominal}$, a limitation in Q is not taken into account[10].

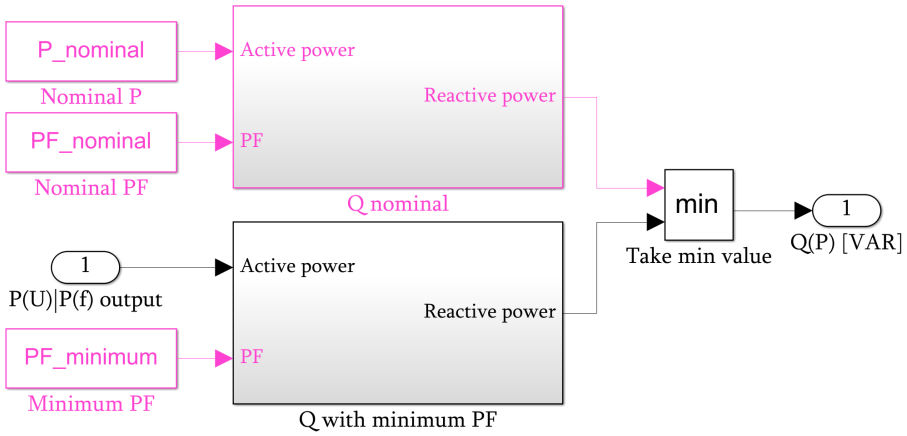

Figure 32: Q(P) mode using $PF_{minimum}$ and $Q_{nominal}$

4.6.2 Q(P) mode 2

The second mode uses a varying PF as a function of P output. Figure 33 illustrates that the PF varies from 0.9 to 1. The slope from 0.5 to 1.0 p.u. P can be changed according to DSO or local requirements.

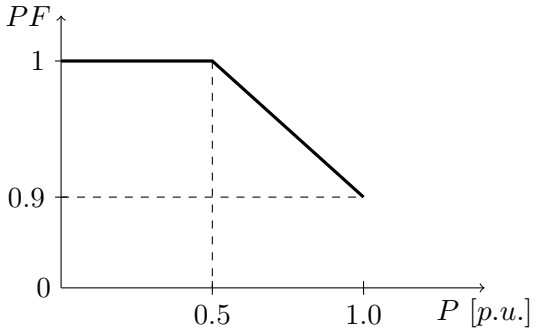

Figure 33: PF(P) characteristic

Figure 34 is the actual implementation in Simulink. The calculated PF is then used together with $P_{available}$ to calculate the Q(P) output. The saturation block acts as a limiter. Output values are limited to possible values defined inside the PF(P) characteristic.

[10] the limitation being the availability factor, depending on sunlight, et cetera

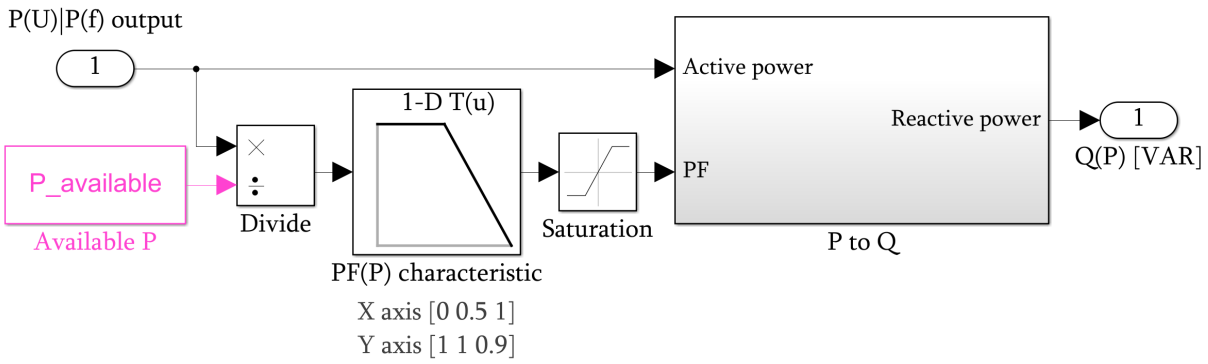

Figure 34: Q(P) mode using PF(P) characteristic implemented in model

4.6.3 Q(P) mode 3

The third mode, shown in Figure 35, uses $PF_{nominal}$ to calculate the Q(P) output. In this mode, the Q output is always proportional to the P output.

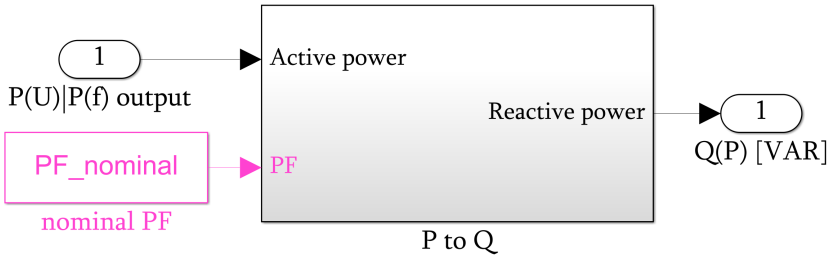

Figure 35: Q(P) mode using $PF_{nominal}$

4.6.4 Q(P) mode 4, 5 and 6

The remaining three modes are the following:

- $Q_{nominal}$ calculated with $PF_{nominal}$ and $P_{nominal}$,
- constant Q,
- zero Q when no Q support is expected.

All six modes will have a different impact on voltage levels. The best mode will differ according to the situation and the general voltage profile of the feeder. Currently, the preferred mode is chosen manually to better evaluate the impact in specific situations. Selecting the Q-mode with the lowest Q output will be beneficial for the PV owner, but less beneficial for supporting voltage and frequency levels at the POC.

4.7 Q(U) characteristic

The output of the Q-mode selector is used to calculate the actual Q output. This calculation is done using a Q(U) characteristic, shown in Figure 36 and implemented in Figure 37. It is important to note that this characteristic presumes the presence of energy storage (negative values indicate absorbing Q) . This characteristic can also be adapted to be used without energy storage, but this will have an impact on the results when overvoltage is present. It will not be possible to absorb Q, the upper voltage level at the POC may be exceeded more often and the P(U) characteristic will be activated more often.

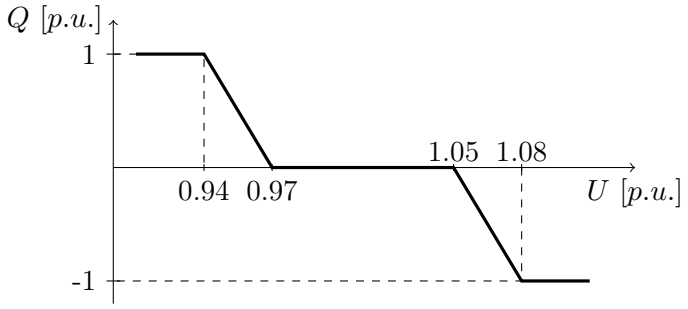

Figure 36: Q(U) characteristic

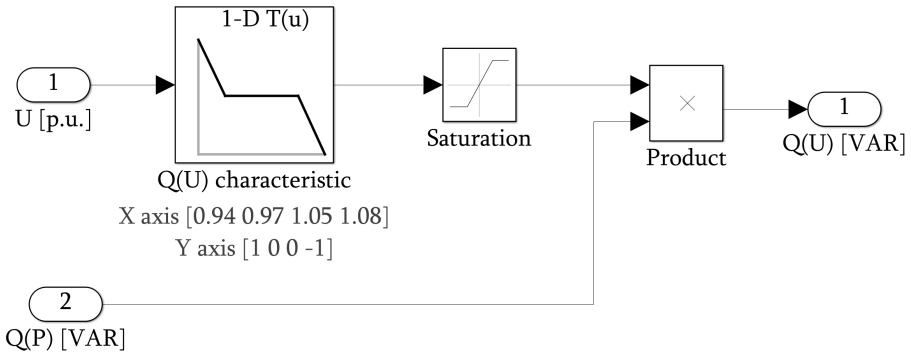

Figure 37: Q(U) characteristic implemented in model

4.8 The use of time constants in the P(U), P(f) and Q(U) characteristics

Inverters can deliver instantaneous power and this can cause more imbalance. Wind turbines, on the other hand, have a mass inertia that prevents instantaneous changes. To imitate this for inverters, time constants are implemented. The P(U), P(f) and Q(U) characteristics use a different time constant. This time constant is changed manually, but in real life operation this time constant is requested by the relevant DSO. A basic method for setting up a discrete transfer function is shown in Figure 38. The c2d (continuous to discrete) command calculates the discrete equivalent of a continuous time transfer function. The disp (display) command returns the zeros, poles, gain and other data. This method is useful when using a fixed time constant, but for time constants requested by DSOs, a more complex method is used to calculate the discrete transfer function.

```
s = zpk(0, [], 1);                  %define s as a state variable
continuous = 1/(0.4*s+1);
discrete = c2d(continuous, 0.02);
disp(discrete);
%output:
  zpk with properties:
                Z: {[0x1 double]}   %zeros
                P: {[0.9512]}       %poles
                K: 0.0488           %gain
         Variable: 'z'              %z domain
               Ts: 0.0200           %sample time
```

Figure 38: A basic method for continuous to discrete time domain

To offer more flexibility regarding time constants, the Model Discretizer (Simulink app), shown in Figure 39, is used. A continuous time transfer function can be configured and is used to compute the discrete transfer function. The zero-order hold (ZOH) method, shown in Figure 41(a), is chosen since this method uses the exact continuous value and holds it for (in this case) 0.02 s. This is illustrated in detail in Figure 41(b).

The possibility of changing the time constant, even during simulation, is interesting for comparing the impact of different time constants. Also, this can simulate the input of DSOs. As above-mentioned, a specific time constant can be requested by the DSO to influence the impact of the DER. Since P(U) as well as P(f) can determine the calculated P output, it is necessary to add a function which uses the same conditions as the P(U)|P(f) output (minimum between P(U) and P(f), unless U is below 0.94 [p.u.], always use P(U) output). The implementation method is shown and further explained in Figure 40.

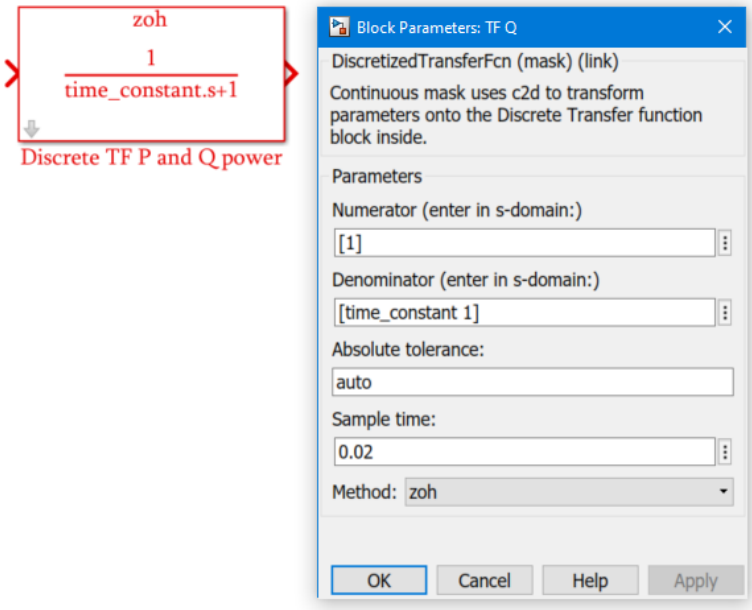

Figure 39: Continuous to discrete using ZOH and a variable time constant

```
function fcn(tc_PU, tc_Pf, tc_QU, connect, upu, pu, pf)
% tc = time constant, connect = boolean (cb open or ROCOF violation?)
% upu = U [p.u.], pu = P(U) value, pf = P(f) value
coder.extrinsic('get_param')
coder.extrinsic('assignin')
mdlWks = get_param('model_v3_SinglePhase','ModelWorkspace'); %get variables

persistent n

if isempty(n) % initialize n
    n = 0;
end

if connect == false && n == 1 % incorrect workaround for cb issues
    assignin(mdlWks,'time_constant_PUf',0.0001);
    assignin(mdlWks,'time_constant_QU',0.0001);
elseif connect == true && upu > 0.94 && pu<=pf
% set P(U)|P(f) time constant according to u and min[P(U),P(f)] conditions
    assignin(mdlWks, 'time_constant_PUf', tc_PU);
% set Q(U) time constant
    assignin(mdlWks,'time_constant_QU',tc_QU);
% reset variable
    n = 0;
elseif connect == true && upu > 0.94 && pu>pf
    assignin(mdlWks, 'time_constant_PUf', tc_Pf);
    assignin(mdlWks,'time_constant_QU',tc_QU);
    n = 0;
elseif connect == true && upu <= 0.94
    assignin(mdlWks, 'time_constant_PUf', tc_PU);
    assignin(mdlWks,'time_constant_QU',tc_QU);
    n = 0;
end

if connect == true && n == 0
   % when fault happens, wait until next time step to change time constant
    n = 1;
end
```

Figure 40: The method for changing the time constants according to P(U) or P(f) output

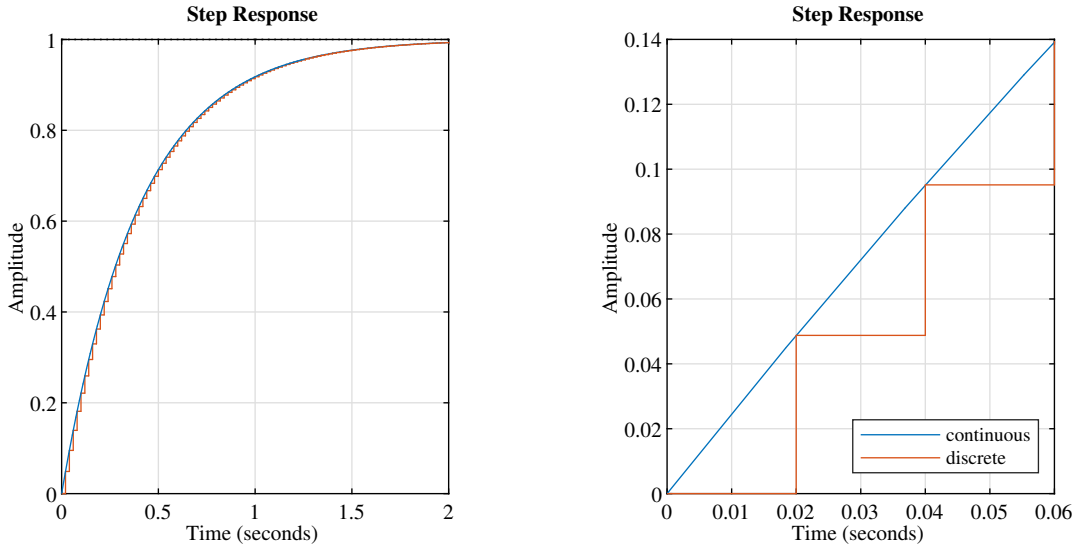

(a) (b)

Figure 41: ZOH: (a) normal view and (b) zoomed view

4.9 Fault-ride-through and model protection

An important fault-ride-through (FRT) capability is ROCOF tripping. According to the standards and regulations [6], the ROCOF must be measured in a *sliding* measurement window of 500 ms. As shown in Figure 42, the actual frequency is evaluated using an array of 25 values, since the sample time of the simulation model is 20 ms.

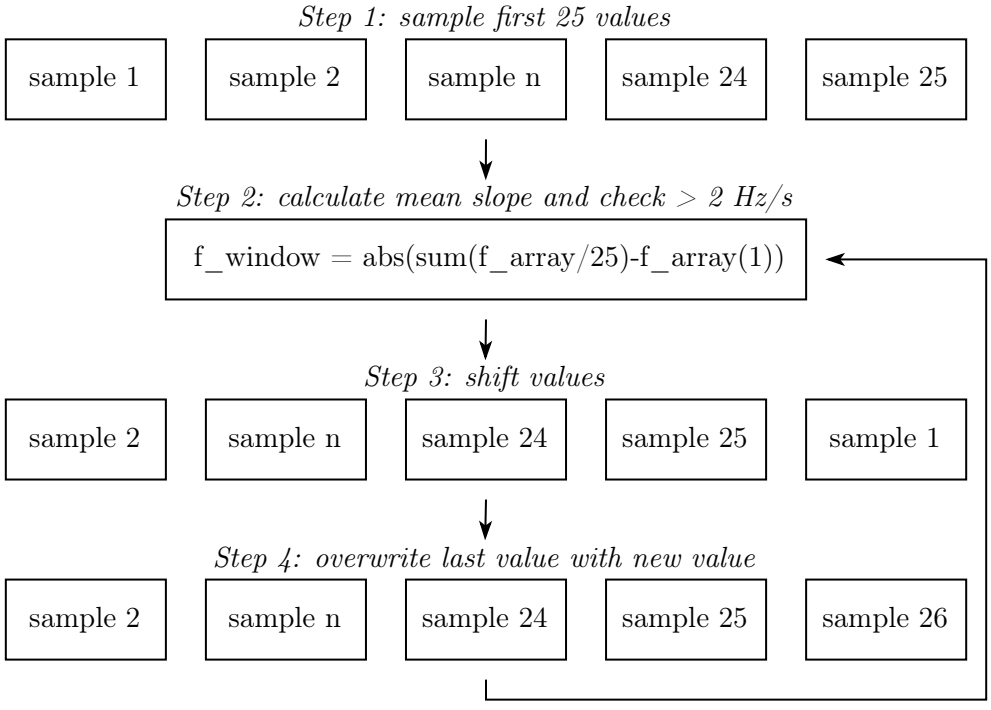

Figure 42: The basic principle of evaluating ROCOF using a sliding window measurement of 500 ms

The actual implementation is depicted in Figure 43. First, the *isemtpy* if-statement is used to initialize the counter n, array f_array and boolean rocof_violation. Second, the array is filled with the first 25 values. This only happens at the start of the simulation. Last, the array is shifted one position so that the measurement window is 'sliding'. The first value becomes the last value and is overwritten with a new sample value.

```
function y = fcn(f_actual)

persistent f_array
persistent n
persistent f_window
persistent rocof_violation

    if isempty(n)
        n = 1;
        f_array = zeros(1,25);
        rocof_violation = false;
    end

    if n<=25
        f_array(n) = f_actual;
    end

    if n >= 26
        f_window = abs(sum(f_array/25)-f_array(1));

        if f_window > 1
            rocof_violation = true;
        else
            rocof_violation = false;
        end

        f_array = circshift(f_array,-1);
        f_array(25) = f_actual;
    end

    n = n+1;
    y = rocof_violation;
```

Figure 43: The implementation of ROCOF using a sliding window measurement of 500 ms

To prevent the PV inverter from disconnecting and reconnecting instantly, a time delay for reconnecting can be applied, as shown in Figure 44. For the example in Figure 45, a time delay of two seconds is set. Two seconds is only for example purposes and is not a regulation. This time delay is applied after a ROCOF violation or after disconnecting the PV inverter manually.

```
function y = fcn(clock, cb, rocof_violation) % cb = circuit breaker status
persistent clock_start      % time when disconnect or ROCOF violation happens
persistent clock_present    % current simulation time
persistent output
persistent wait_period;

if isempty(clock_start)
    clock_start = 0;
    output = 1;
    wait_period = false;
end

clock_present = clock;

if cb == 0 || rocof_violation == 1
    clock_start = clock;
    wait_period = true;
end

if wait_period == true && (clock_present - clock_start) >= 2
   output = 1;
   wait_period = false;
elseif wait_period == true && (clock_present - clock_start) < 2
   output = 0;
end

y = output;
```

Figure 44: Code for a time delay of 2 seconds for reconnecting after a ROCOF violation or a (manual) disconnect

Without this layer, the simulation model will stay connected, even if values are calculated or measured which can possibly harm the hardware. To prevent this from happening, FRT capabilities are implemented via software to respect hardware limits and maximum required capabilities.

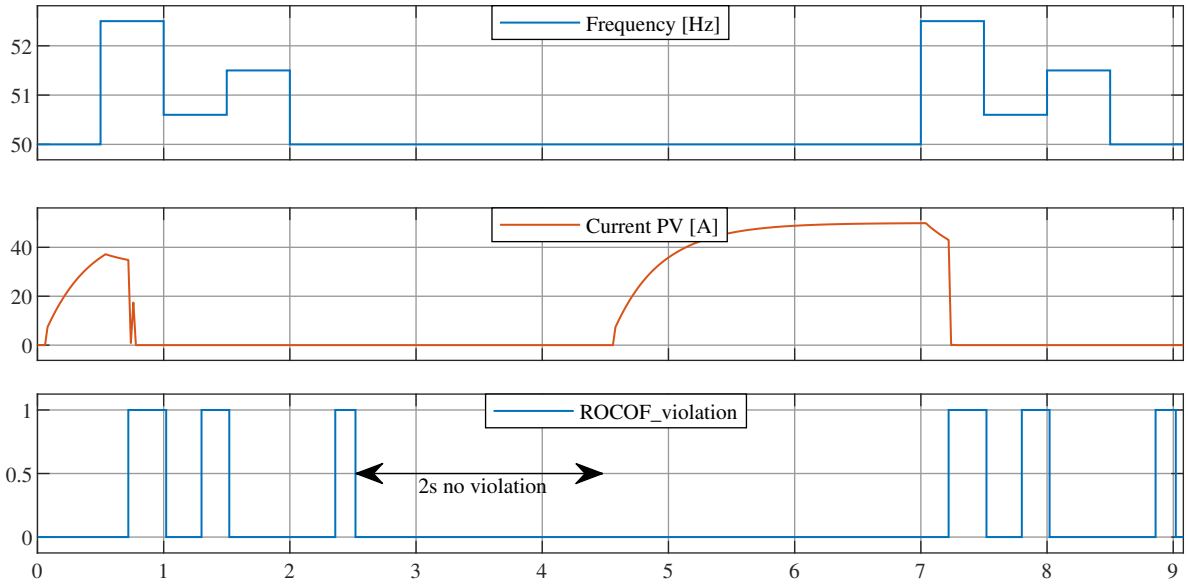

Figure 45: ROCOF violation with a time delay of 2 seconds for reconnecting to the grid

When the circuit breaker is open, the voltage measurement in Figure 25 will output Not a Number (NaN). This will cause the model to crash since further calculations cannot be made correctly. To prevent this from happening, a straightforward solution, as shown in Figure 46, can be applied. If the value 'voltage_in' is NaN, it will be converted to zero. This method is also implemented for the current measurement block in Figure 25.

```
function voltage_out = fcn(voltage_in)

voltage_in(isnan(voltage_in)) = 0;

voltage_out = voltage_in;
```

Figure 46: Converting NaN to zero to protect the simulation model from crashing

4.10 Case studies for validation

To validate the implemented MATLAB functions, P(U), P(f), Q(P) and Q(U) characteristics, specific tests are performed to explain the output and indicate the accuracy of implementation. Table 6 summarizes the test conditions. These are valid for all four case studies.

Table 6: Model settings used in the case studies

Description	Value or setting
$PF_{nominal}$	0.90
$PF_{minimum}$	0.85
Q mode	Q mode 1 (see 4.6.1)
$P_{nominal}$	10.00 kW
$P_{available}$	1.00 p.u.
P(U) τ	0.40 s
P(f) τ	0.40 s
Q(U) τ	0.40 s
Main source voltage	414.00 V
Line length	1.00 km
Extra two loads	Both off
Overvoltage setpoints	[1.00 1.05 1.09 1.10 1.11]
Undervoltage setpoints	[1.00 0.98 0.96 0.94 0.92]
Voltage error	0.00 %
Overfrequency setpoints	[50.00 50.50 51.10 50.50 50.00 50.00]
Underfrequency setpoints	[50.00 49.80 49.50 49.00 50.00 50.00]
Frequency error	0.00 Hz

Three cases were chosen to perform the validation and are indicated in Table 7. The choice for not testing underfrequency was made since underfrequency support is not provided by Type A and Type B PGMs.

Table 7: The four chosen cases for performing the case studies

	over f	**constant f**	**under f**
over U	4.10.4 & Figure 50	4.10.1 & Figure 47	
constant U	4.10.2 & Figure 48		
under U	4.10.3 & Figure 49		

The following figures are highlighted with time stamps. These time stamps indicate interesting points and are explained in the corresponding table. The X value indicates the time in seconds and the Y value indicates the corresponding value depicted in the legend of the figure.

4.10.1 Case 1: overvoltage with constant frequency

Figure 47 is used to indicate the functioning of the P(U) characteristic (see Figure 26). Table 8 summarizes the interesting points.

Table 8: Interesting points for overvoltage with constant frequency

Time stamp	Description
4.20 s	Voltage exceeds 1.09 p.u. which activates the P(U) characteristic. P output (and therefore also Q output) drop accordingly.
6.04 & 8.04 s	Voltage reaches 1.11 p.u., P and Q drop accordingly to mitigate the overvoltage violation.
8.28 s	Voltage drops below 1.11 p.u. so P and Q output can increase.
10.00 s	Voltage drops below 1.09 p.u. so P and Q output are not limited by the P(U) characteristic anymore.

4.10.2 Case 2: constant voltage with overfrequency

Figure 48 indicates the functioning of the P(f) characteristic and when voltage drops below 0.94 p.u., the P(f) characteristic is blocked so only the P(U) characteristic can determine the calculated P. Table 9 summarizes the interesting points.

Table 9: Interesting points for constant voltage with overfrequency

Time stamp	Description
2.00 s	Overfrequency occurs, P(f) characteristic is activated to limit P output.
7.30 s	Voltage drops below 0.94 p.u., this indicates that the P(f) characteristic is blocked and only the P(U) characteristic determines the P calculated.
8.00 s	The overcurrent limit is reached (10 % overcurrent) at 55 A. This is a good indication that the calculated P and actual P output are not always necessarily the same. At this point, P and P output are limited to protect the hardware from providing too much current.

4.10.3 Case 3: undervoltage with overfrequency

Figure 49 is used to depict the blocking of the P(f) characteristic when the voltage level is 0.94 p.u. or lower. This blocking is implemented to prevent a bigger voltage drop when both undervoltage and overfrequency are present at the same time. Table 10 summarizes the interesting points.

Table 10: Interesting points for undervoltage and overfrequency at the same time

Time stamp	Description
2.00 s	Overfrequency occurs, P output drops according to P(f) characteristic.
4.14 s	Voltage drops below 0.94 p.u., P(f) characteristic is blocked and P(U) characteristic determines calculated P.
4.58 s	Overcurrent limit is reached. Calculated and actual P and Q differ from each other.

4.10.4 Case 4: overvoltage with overfrequency

Figure 50 depicts the use of the minimum between P(U) and P(f) characteristics when voltage level is 0.94 p.u. or higher. During the entire simulation time, the P(U) characteristic outputs less P and is therefore determining the calculated P output. The interesting points in Table 11 are similar to overvoltage with constant frequency, as the P(f) characteristic is not used here.

Table 11: Interesting points for overvoltage and overfrequency at the same time

Time stamp	Description
2.00 s	Overfrequency occurs, P output drops according to P(f) characteristic.
4.38 s	Voltage exceeds 1.09 p.u. which activates the P(U) characteristic. P output (and therefore also Q output) drop accordingly.
6.04 & 8.04 s	Voltage reaches 1.11 p.u., P and Q drop accordingly to mitigate the overvoltage violation.
8.28 s	Voltage drops below 1.11 p.u. so P and Q output can increase.

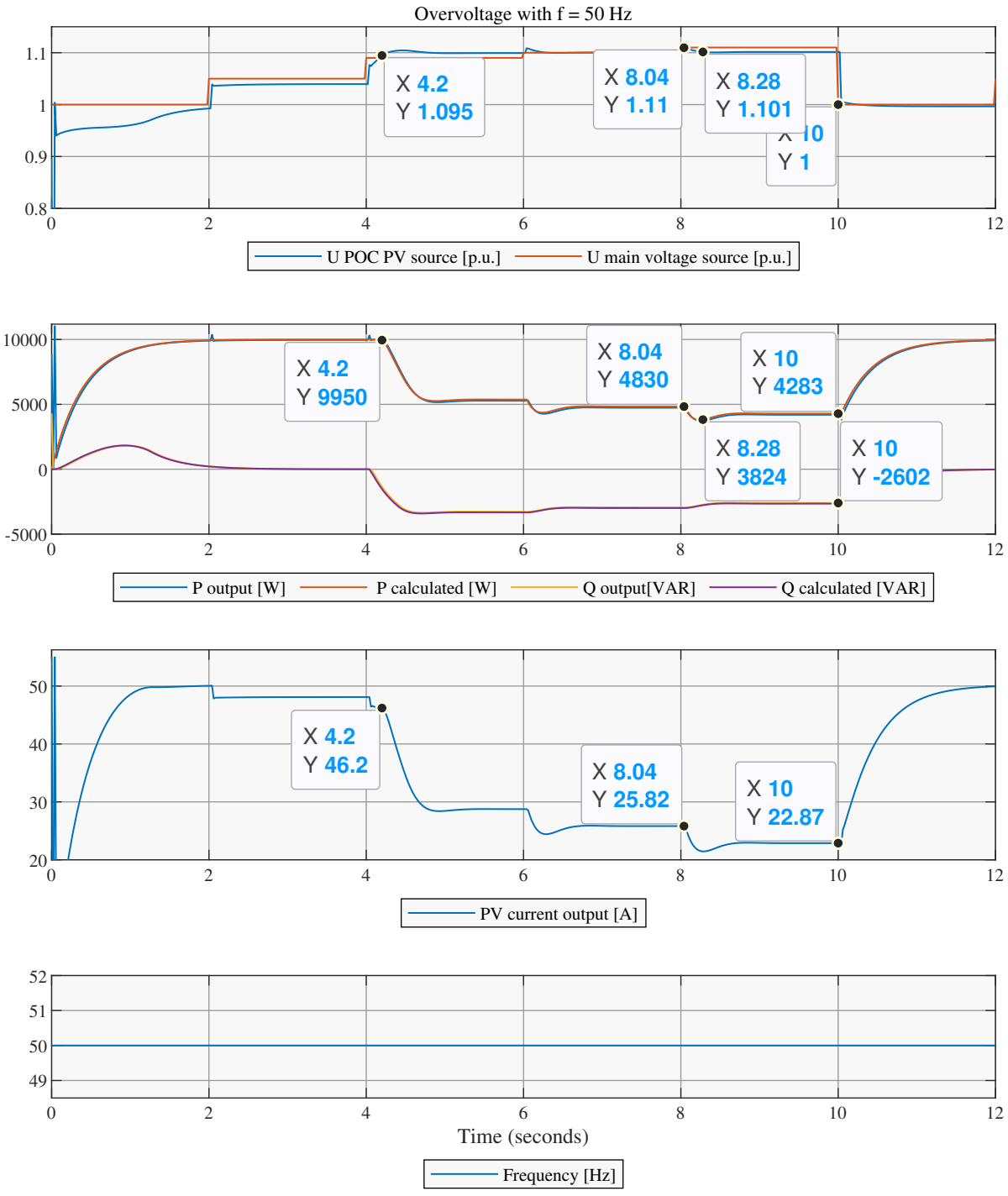

Figure 47: Case 1: overvoltage and constant frequency

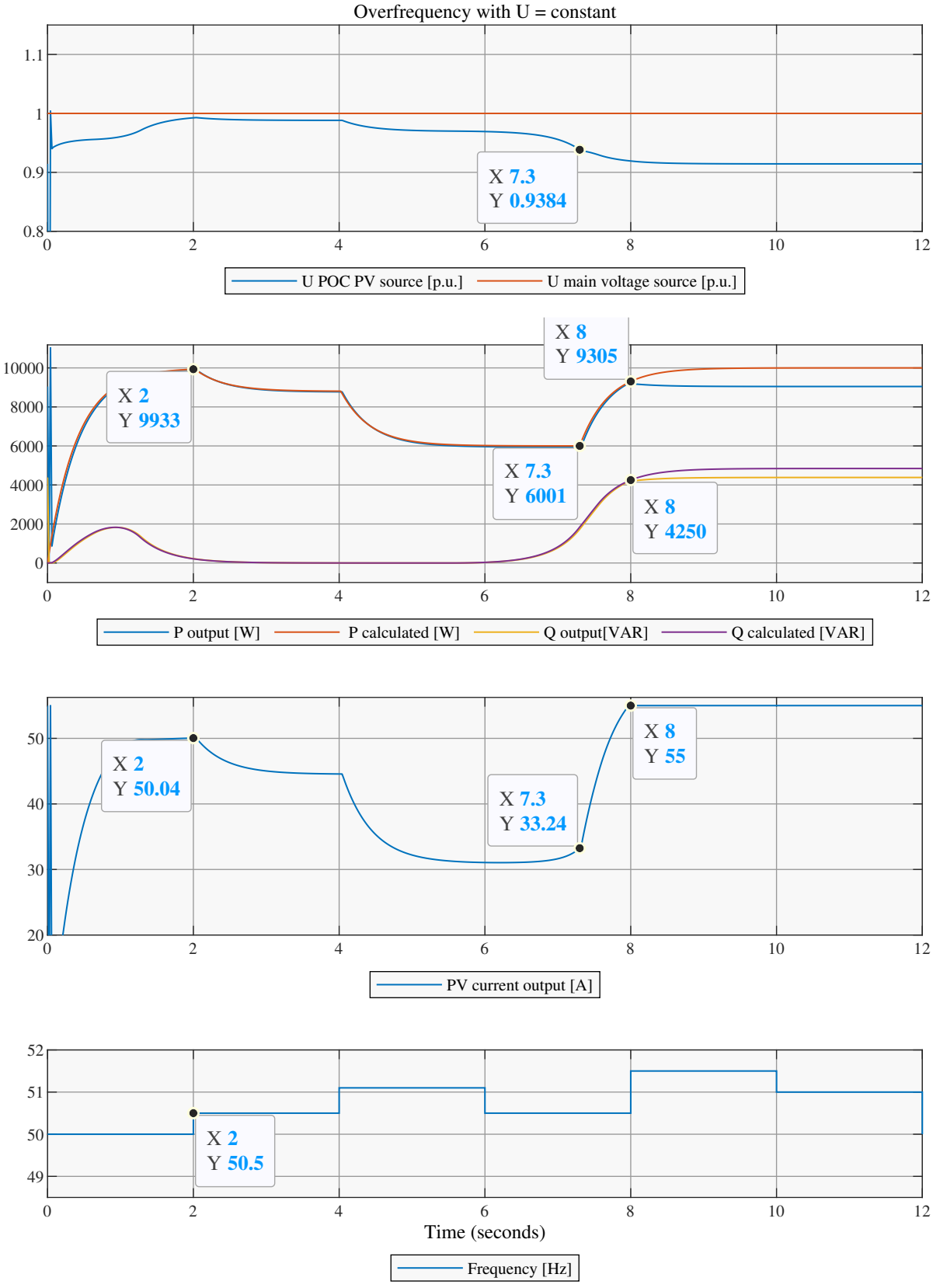

Figure 48: Case 2: constant voltage and overfrequency

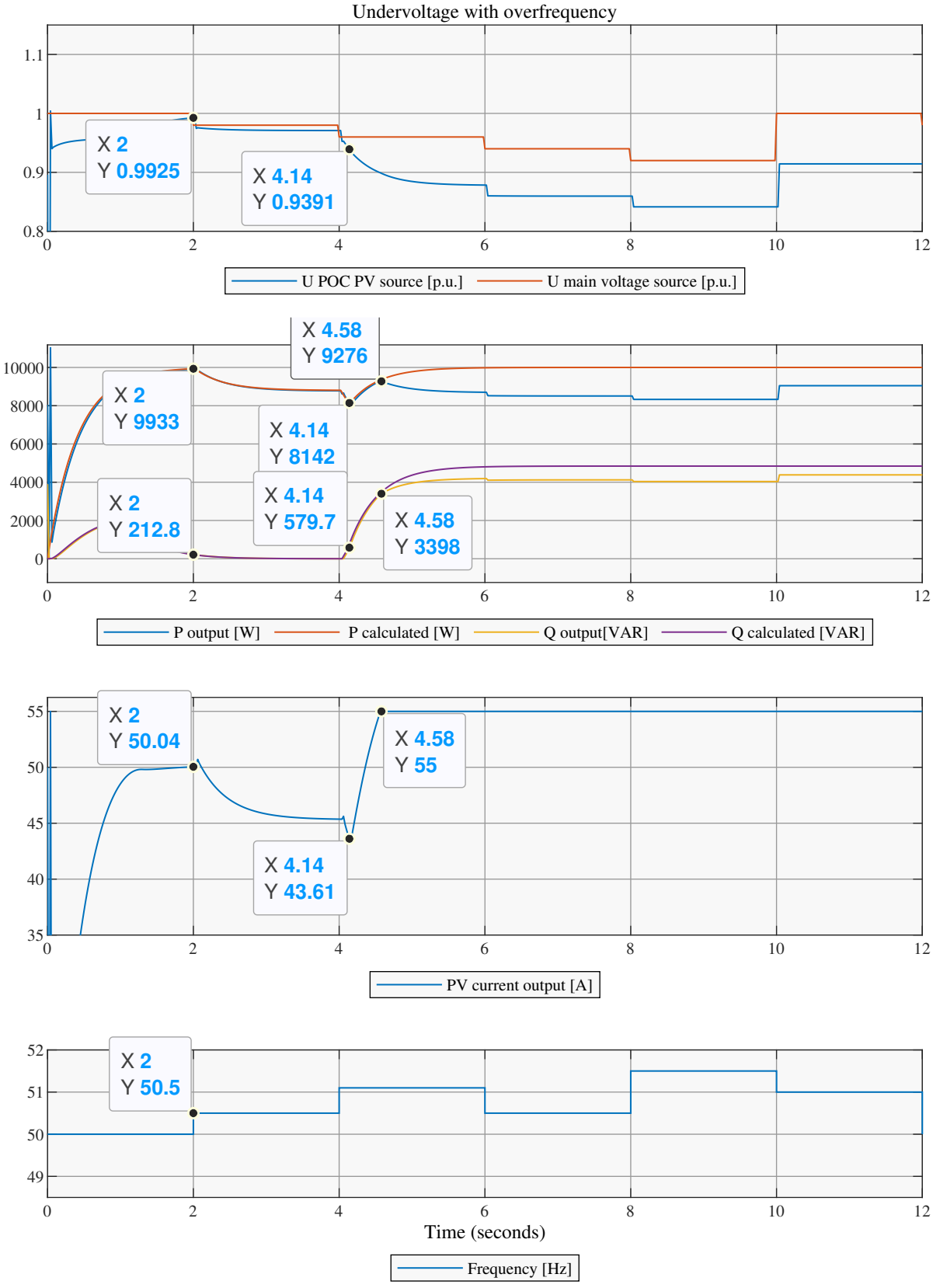

Figure 49: Case 3: undervoltage and overfrequency

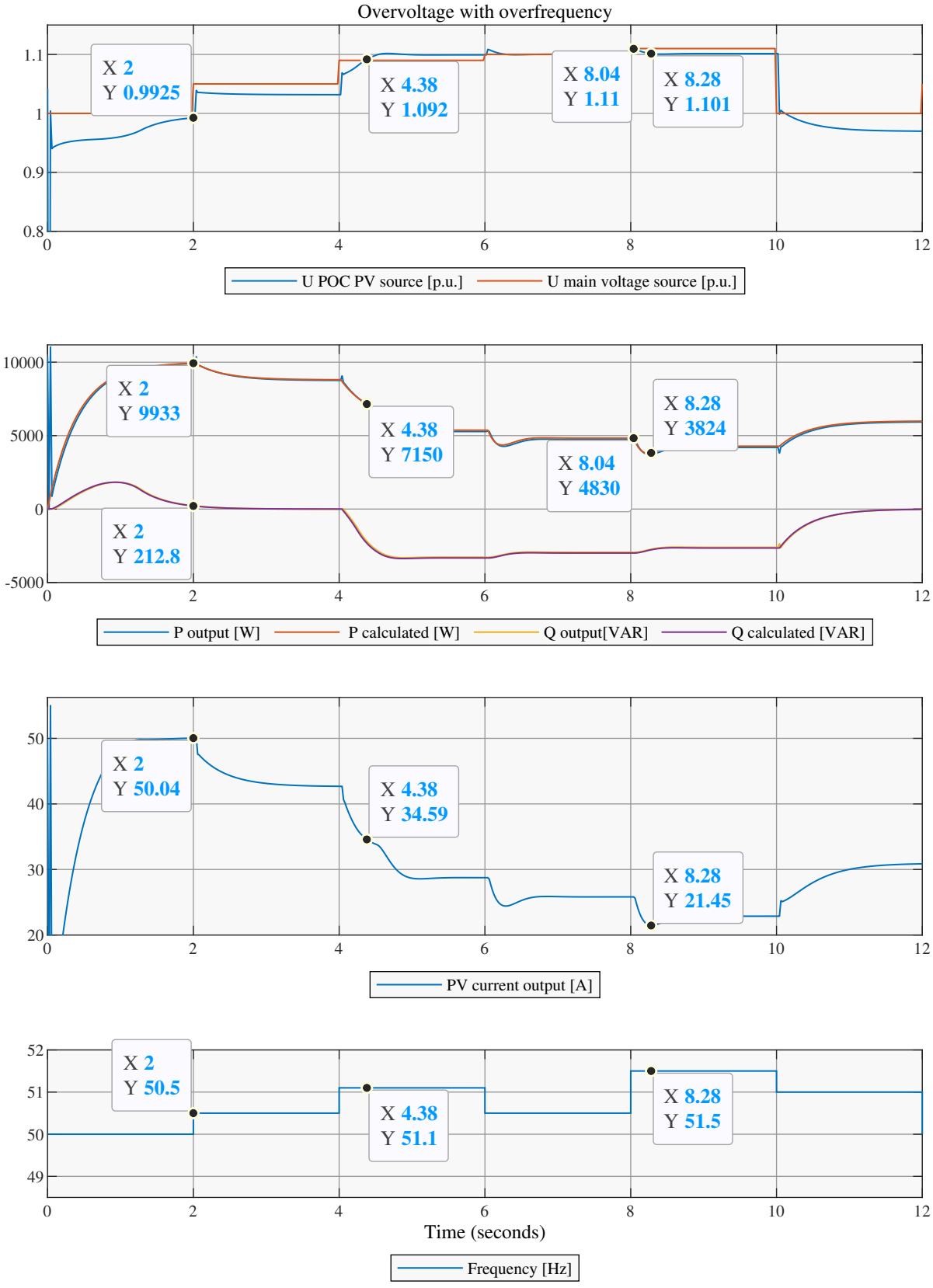

Figure 50: Case 4: overvoltage and overfrequency

5 Conclusions

5.1 Main conclusions

For a long time, OLTCs has been the only mechanism to change local voltage levels. Unfortunately, they do not suffice anymore because voltage levels in different feeders are controlled by the same OLTC. Therefore, extra support is needed. Inverters can be used, but current drawbacks, such as the lack of simulation models, make them difficult to implement. DSM has many requirements that have to be met. Also, it requires a great effort, technological and participation-wise, in order to successfully provide flexibility. Nonetheless, Linear was a project which provided many details, results and recommendations for future projects. Given that none of the above-mentioned methods can be used as a standalone solution, it can be concluded that a combination of these methods should be implemented [24]. This thesis provides more insight and solutions for simulating the integration of inverter-based DERs into the grid by developing a simulation model in MATLAB / Simulink.

The focus on PV is due to its variety in large scale as well as household applications. Households are supplying an amount of power which can no longer be ignored. As a result, voltage deviations are occurring more frequently and with a higher amplitude, but only impacts the local grid [10]. Instead of reinforcing the grid, PV inverters can become an important part of grid support. For this reason, standards and regulations should be implemented. While PV is a clean alternative, it is only contributing for 2.9 % of the global electricity demand. This indicates that PV still has several challenges to overcome in order to become a comprehensive solution to abandon polluting power generation facilities. Ultimately, the development in energy storage (electrical, thermal, hydrogen, etc.) can play an important role in stimulating investments in RERs in general.

When looking back at chapter 3, the requirements for over- and underfrequency do not guarantee an adjustment in voltage levels since the available P of the inverter depends on uncontrollable variables, i.e. the amount of sunlight in case of a PV inverter. Therefore, type A PGMs can merely be used as an extra control since its impact is considered insufficient. The possibility of modifying P output as a function of voltage has not been discussed as this is considered a basic functionality. Type B PGMs will have a greater impact, while they also provide voltage support by modifying P or Q. Q is used to control voltage levels in grids where the reactance X has a significant impact. This is primarily the case in MV grids. Given the above, it can be concluded that LV grid support will affect the inverter-based DER owner. By reducing the P output, the income for the owner will be less. On the other hand, providing grid support also makes sure that the limits are violated less often and the PGM remains connected over a longer period of time. In general, the requirements will have a positive impact on the grid and the DER owner.

(See back)

5.2 Recommendations and future work

It is advised to add a MATLAB script which changes the time constants according to dP/dt and dQ/dt. When the slope is 100 W/s, it will take as long as 1000 W/s (it takes 5 τ in both cases to output the change). Implementing this automatic adjustment will allow smaller changes to output faster.

The implementation of a circuit breaker posed some issues. It did not interact with the rest of the simulation model (the current source in specific), which made it necessary to add a workaround. The status of the circuit breaker is used to stop current output, when normally there should be no current output when there is no closed circuit. This has to be reworked or fixed as soon as MATLAB provides a correct solution. The workaround for the circuit breaker made the model more complex than it should be. When this is solved, the model can be further simplified to improve simulation time.

Another issue encountered is due to using the phasor method; it assumes a fixed model frequency. Therefore, the P(f) characteristic uses a manual frequency input to trigger the characteristic.

5.3 Contributions

The main contributions of this thesis are the following items:

- a comprehensive summary of the state-of-the-art grid support and control technology, and European standards and regulations;
- a simulation model for modelling the impact of DERs in LV grids with respect to standards and regulations using the phasor method;
- a method for changing time constants in the discrete time domain whilst respecting P(U) or P(f) conditions;
- a method for frequency value thresholding in case of overfrequency;
- a method for evaluating ROCOF in a sliding window measurement.

By using case studies, it was found that the model performs as expected and can be used for further development. Using MATLAB / Simulink is a well established method for modelling the impact of DERs on LV grids. The phasor method showed that it can perform well in conditions with computational complexity. Writing this thesis gave me great insight in the possibilities with Simulink and the necessary steps to take when starting a new project. The literature study provided me with a strong basis and an overview of the state-of-the-art technology.

References

[1] C. Dierckxsens, *METAPV: technical project overview and results*, Accessed 31 December 2019, Brussels, Belgium, 2015. [Online]. Available: http://www.metapv.eu/sites/default/files/PR_PR104282_FullProjectReport_F.pdf.

[2] T. Fawzy, D. Premm, B. Bletterie, and A. Goršek, "Active contribution of PV inverters to voltage control-from a smart grid vision to full-scale implementation", *Elektrotechnik & Informationstechnik*, vol. 128, no. 4, pp. 110–115, 2011. DOI: 10.1007/s00502-011-0820-z.

[3] K. Yamashita, "Modelling of inverter-based generation for power system dynamic studies", CIRED Joint Working Group, Tech. Rep., 2018.

[4] R. Belmans, "Linear, Demand Response for Families", EnergyVille, Genk, Belgium, Tech. Rep., 2014.

[5] G. Masson and I. Kaizuka, "Trends in photovoltaic applications", IEA PVPS, Tech. Rep., 2019.

[6] "Commission regulation (EU) of 14 April 2016/631 establishing a network code on requirements for grid connection of generators", *Official Journal of the European Union*, Apr. 2016.

[7] CENELEC, "EN 50549-2:2018 Requirements for generating plants to be connected in parallel with distribution networks - Part 2: Connection to a MV distribution network - Generating plants up to and including Type B", 2018.

[8] K. N. Malamaki and C. S. Demoulias, "A decentralized voltage regulation method in low-voltage feeders with PV systems and domestic loads", *International Conference on Power Engineering, Energy and Electrical Drives*, no. 4, pp. 461–467, 2013, ISSN: 21555516. DOI: 10.1109/PowerEng.2013.6635652.

[9] MathWorks, *Introducing the Phasor Simulation Method*, Accessed 10 February 2020. [Online]. Available: https://nl.mathworks.com/help/physmod/sps/powersys/ug/introducing-the-phasor-simulation-method.html.

[10] A. Dexters, *Energiebeheersystemen: Voltage control [course]*. Diepenbeek, Belgium: Gezamenlijke opleiding Industriële Ingenieurswetenschappen UHasselt & KU Leuven, 2019.

[11] S. Weckx, C. González de Miguel, T. De Rybel, and J. Driesen, "LS-SVM-based On-Load Tap Changer Control for Distribution Networks with Rooftop PV's", in *Innovative Smart Grid Technologies Europe (ISGT Europe)*, Copenhagen, Denmark: IEEE, 2013, pp. 1–5. DOI: 10.1109/ISGTEurope.2013.6695229.

[12] N. Efkarpidis, T. Wijhoven, C. González de Miguel, T. De Rybel, and J. Driesen, "Coordinated voltage control scheme for Flemish LV distribution grids utilizing OLTC transformers and D-STATCOM's", in *IET Conference Publications*, 2014, pp. 1–6.

[13] A. Q. Al-Shetwi, M. Z. Sujod, and F. Blaabjerg, "Low voltage ride-through capability for single-stage inverter-based grid-connected photovoltaic power plant", *Solar Energy*, vol. 159, pp. 665–681, 2018. DOI: https://doi.org/10.1016/j.solener.2017.11.027.

[14] F. Famoso, R. Lanzafame, S. Maenza, and P. F. Scandura, "Performance comparison between micro-inverter and string-inverter Photovoltaic Systems", in *Italian Thermal Engineering Association (ATI)*, vol. 81, Catania, Italy, 2015, pp. 526–539. DOI: 10.1016/j.egypro.2015.12.126.

[15] S. K. Chattopadhyay and C. Chakraborty, "Photovoltaic central inverters: Performance evaluation and comparative assessment", in *Proceedings IECON 2017 - 43rd Annual Conference of the IEEE Industrial Electronics Society*, vol. 2017-January, Institute of Electrical and Electronics Engineers Inc., Dec. 2017, pp. 6419–6424, ISBN: 9781538611272. DOI: 10.1109/IECON.2017.8217118.

[16] S. Harb, M. Kedia, H. Zhang, and R. S. Balog, "Microinverter and string inverter grid-connected photovoltaic system — A comprehensive study", in *2013 IEEE 39th Photovoltaic Specialists Conference (PVSC)*, 2013, pp. 2885–2890. DOI: 10.1109/PVSC.2013.6745072.

[17] A. B. Nassif, T. Greenwood-Madsen, S. P. Azad, and D. F. Teshome, "Feeder Voltage Management through Smart Inverter Advanced Functions and Battery Energy Storage System", in *IEEE Power and Energy Society General Meeting*, vol. 2018-August, IEEE Computer Society, Dec. 2018, ISBN: 9781538677032. DOI: 10.1109/PESGM.2018.8586083.

[18] J. Huang, W. Ziqiang, D. Zhihao, and Y. Zhu, "Photovoltaic Single-Phase Grid-Connected Inverter Based on Voltage and Reactive Power Support", *Materials Science and Engineering*, vol. 366, p. 012 014, 2018. DOI: 10.1088/1757-899X/366/1/012014.

[19] S. Gottwalt, W. Ketter, C. Block, J. Collins, and C. Weinhardt, "Demand side management — A simulation of household behavior under variable prices", *Energy Policy*, vol. 39, no. 12, pp. 8163–8174, 2011. DOI: https://doi.org/10.1016/j.enpol.2011.10.016.

[20] "Spaarbekkencentrale Coo: Elektriciteit produceren uit water", Electrabel n.v., Brussels, Belgium, Tech. Rep., 2016, pp. 1–24.

[21] Solenco Power NV, *Energy for the new era*, Accessed 20 April 2020. [Online]. Available: www.solencopower.com.

[22] CREG, *Strategische reserve*, Accessed 13 April 2020. [Online]. Available: https://www.creg.be/nl/professionals/marktwerking-en-monitoring/strategische-reserve.

[23] C. Castillo Perpiña, "An assessment of the regional potential for solar power generation in EU-28", *Energy Policy*, vol. 88, pp. 86–99, 2016. DOI: https://doi.org/10.1016/j.enpol.2015.10.004.

[24] J. Hu, M. Marinelli, M. Coppo, A. Zecchino, and H. W. Bindner, "Coordinated voltage control of a decoupled three-phase on-load tap changer transformer and photovoltaic inverters for managing unbalanced networks", *Electric Power Systems Research*, vol. 131, pp. 264–274, 2016. DOI: https://doi.org/10.1016/j.epsr.2015.10.025.